REPORT SERIES IN AEROSOL SCIENCE
N:o 90 (2007)

INVESTIGATIONS OF PLANETARY BOUNDARY LAYER PROCESSES AND PARTICLE FORMATION IN THE ATMOSPHERE OF PLANET MARS

ANNI MÄÄTTÄNEN

Division of Atmospheric Sciences
Department of Physical Sciences
Faculty of Science
University of Helsinki
Helsinki, Finland

Academic dissertation

To be presented, with the permission of the Faculty of Science of the University of Helsinki, for public criticism in Chemicum auditorium A110, A. I. Virtasen aukio 1, on 23rd November, 2007, at 12 o'clock.

Helsinki 2007

ISBN 978-952-5027-84-6 (printed version)
ISSN 0784-3496
Helsinki 2007
Yliopistopaino

ISBN 978-952-5027-85-3 (pdf version)
http://ethesis.helsinki.fi
Helsinki 2007
Helsingin yliopiston verkkojulkaisut

Acknowledgements

The work presented in this thesis has required time, space and hardware, and my gratitude goes to the Head of Department of Physical Sciences, Prof. Juhani Keinonen, for providing me with the facilities of Physicum, and to the Finnish Meteorological Institute Director General, Pekka Plathan, and the Chief of the Space Research Unit, Dr. Tuija I. Pulkkinen, for placing the facilities of Dynamicum at my disposal. I also sincerely thank the Head of Division of Atmospheric Sciences, Prof. Markku Kulmala, for giving me the possibility to work in his group and benefit from their pioneering work in aerosol research even though I insisted on staying on another planet.

I am indebted to my supervisors, Prof. Hannu Savijärvi and Dr. Hanna Vehkamäki. I thank Prof. Savijärvi for giving me the chance to proceed with my interest in meteorology of Mars and sharing his innovative ideas on 1-D modelling with me. Dr. Vehkamäki has been a brilliant, encouraging guide to science, nucleation, and everything: I want to express her my deepest gratitude.

I thank the reviewers of my thesis, Dr. Stephen E. Wood and Dr. Franck Montmessin for very good, constructive comments, and their encouragement.

I wish to thank my co-authors Dr. Ari-Matti Harri, Mr. Janne Kauhanen, Ms. Sini Merikallio, Dr. Antti Lauri and Dr. Ismo Napari for their help and support. My gratitude goes particularly to Dr. Lauri for helping me with basics of heterogeneous nucleation, and for his shoulder in the last stages of my thesis. Dr. Tero Siili influenced me a lot during my first years in science. He was always ready to help, discuss, encourage, brainstorm, and laugh with me, and I am very grateful for his continuous support. I sincerely thank the members of the simulation subgroup and its predecessors, and the Mars-group of the FMI and the University of Helsinki for an inspiring working environment.

I also wish to thank financial support from the Academy of Finland, the Alfred Kordelin foundation and the Graduate School in Astronomy and Space Physics. Contributions from the Väisälä foundation, Magnus Ehrnrooth foundation, Wihuri foundation, Emil Aaltonen foundation, and Association Franco-Finlandaise pour la Recherche Scientifique et Technique are gratefully acknowledged.

Last, but not least, I wish to thank my family, and my friends, who always believed in me, supported me, and diverted me to think also other things than Mars. I wish to express my deepest gratitude and love to my partner, Marian, who has kept my feet steadily off the ground, and to my parents, Antero and Anna-Liisa, for their endless support, and their patience for always letting me dwell on whatever passion I had in mind, even though sometimes the astronomy books were bigger than the small girl herself.

This thesis is dedicated with gratitude to my godfather Jukka, the original source of my interest in the stars, and to my four nieces Minttu, Ilona, Miina and Kaisla: I wish them lives full of interesting challenges and wonderful, creative years in the paths they choose to take.

Investigations of planetary boundary layer processes and particle formation in the atmosphere of planet Mars

Anni Elisa Määttänen
University of Helsinki, 2007

Abstract

The planet Mars is the Earth's neighbour in the Solar System. Planetary research stems from a fundamental need to explore our surroundings, typical for mankind. Manned missions to Mars are already being planned, and understanding the environment to which the astronauts would be exposed is of utmost importance for a successful mission. Information of the Martian environment given by models is already now used in designing the landers and orbiters sent to the red planet. In particular, studies of the Martian atmosphere are crucial for instrument design, entry, descent and landing system design, landing site selection, and aerobraking calculations.

Research of planetary atmospheres can also contribute to atmospheric studies of the Earth via model testing and development of parameterizations: even after decades of modeling the Earth's atmosphere, we are still far from perfect weather predictions. On a global level, Mars has also been experiencing climate change. The aerosol effect is one of the largest unknowns in the present terrestrial climate change studies, and the role of aerosol particles in any climate is fundamental: studies of climate variations on another planet can help us better understand our own global change.

In this thesis I have used an atmospheric column model for Mars to study the behaviour of the lowest layer of the atmosphere, the planetary boundary layer (PBL), and I have developed nucleation (particle formation) models for Martian conditions. The models were also coupled to study, for example, fog formation in the PBL. The PBL is perhaps the most significant part of the atmosphere for landers and humans, since we live in it and experience its state, for example, as gusty winds, nightfrost, and fogs. However, PBL modelling in weather prediction models is still a difficult task.

Mars hosts a variety of cloud types, mainly composed of water ice particles, but also CO_2 ice clouds form in the very cold polar night and at high altitudes elsewhere. Nucleation is the first step in particle formation, and always includes a phase transition. Cloud crystals on Mars form from vapour to ice on ubiquitous, suspended dust particles. Clouds on Mars have a small radiative effect in the present climate, but it may have been more important in the past.

This thesis represents an attempt to model the Martian atmosphere at the smallest scales with high resolution. The models used and developed during the course of the research are useful tools for developing and testing parameterizations for larger-scale models all the way up to global climate models, since the small-scale models can describe processes that in the large-scale models are reduced to subgrid (not explicitly resolved) scale.

Keywords: Mars, planetary atmospheres, planetary boundary layer, heterogeneous nucleation, particle formation, numerical modeling

Nomenclature

A_{CN}	surface area of the condensation nucleus
$A_{g,i}$	gas phase activity of component i
b	energy lost from the cluster with collisions of molecules
β	a parameter describing the effect of humidity on buoyancy
C	condensation from vapour to ice
CN	condensation nucleus/nuclei
E	sublimation from ice to vapour
E_0	latent heat flux at the surface
f	Coriolis parameter
F^e	equilibrium concentration of monomers
g	gravitational constant
ΔG	Gibbs free energy of formation
H_0	sensible heat flux at the surface
J	nucleation rate
k	Boltzmann constant
k	von Karman's constant
K_c	eddy diffusion coefficient for scalars
K_h	eddy diffusion coefficient for heat
K_m	eddy diffusion coefficient for momentum
l	mixing length
L	Obukhov length
L_s	areocentric longitude of the Sun
λ	thermal conductivity
m	contact parameter, the cosine of the contact angle
m	mass
M	molecular mass
μ	chemical potential
$\Delta\mu$	difference of chemical potential between liquid and vapour phase in the ambient vapour pressure
N	number of molecules
ppm	parts per million
p	pressure
p_s	surface pressure
p_0	reference pressure
P	nucleation probability
ϕ_m	universal function for momentum
ϕ_c	universal function for scalars
q	energy gained to the cluster with adhered molecules
q	specific humidity

q_{ice}	ice mixing ratio
r_{eff}	effective radius
r^*	radius of the critical cluster
R	gas constant
R_{av}	average growth rate of the cluster
R_{CN}	radius of the condensation nucleus
R_{net}	net radiative flux
Ri	Richardson number
ρ	density
ρc	volumetric heat capacity
ρ_l	density of bulk liquid
σ	surface tension
S	saturation ratio
S_i	saturation ratio of component i
t	nucleation time
τ	dust optical thickness
T	temperature
T_s	surface temperature
θ	contact angle
θ	potential temperature
u	horizontal west-east wind component
u_g	geostrophic west-east wind component
u_*	friction velocity
v	horizontal south-north wind component
v_g	geostrophic south-north wind component
v	molecular volume
x	mole fraction
X_l	liquid mass fraction
z	altitude
z_0	roughness length
Z	Zeldovich non-equilibrium factor
ζ	dimensionless height

Subscripts and superscripts:

CN	condensation nucleus/nuclei
hom	homogeneous
het	heterogeneous
g	gas/vapour
g	geostrophic
i	compound i
j	compound j
l	liquid
s	solid (substrate)
$*$	critical value

Abbreviations:

0-D	zero-dimensional
1-D	one-dimensional
2-D	two-dimensional
3-D	three-dimensional
ASI	Atmospheric Structure Investigation
AU	astronomical unit
CN	condensation nucleus/nuclei
CRISM	Compact Reconnaissance Imaging SpectroMeter
DB	Dyer-Businger
DLR	downwelling longwave radiation
DVD	direct vapour deposition
GCM	general circulation model
GRS	Gamma Ray Spectrometer
HiRISE	High Resolution Imaging Science Experiment
HRSC	High Resolution Stereo Camera
LIDAR	LIght Detection And Ranging
MCD	Mars Climate Database
MCS	Mars Climate Sounder
MER	Mars Exploration Rover
MEx	Mars Express
MGS	Mars Global Surveyor
MOC	Mars Orbiter Camera
MOd	2001 Mars Odyssey
MOLA	Mars Orbiter Laser Altimeter
MPF	Mars Pathfinder
MRO	Mars Reconnaissance Orbiter
NASA	National Aeronautics and Space Administration
OMEGA	Observatoire pour la Minéralogie, l'Eau, les Glaces et l'Activité
PBL	planetary boundary layer
PFS	Planetary Fourier Spectrometer
SD	surface diffusion
SPICAM	SPectroscopy for Investigation of Characteristics of the Atmosphere of Mars
TES	Thermal Emission Spectrometer
THEMIS	Thermal Emission Imaging System
VO1	Viking Orbiter 1
VO2	Viking Orbiter 2
VL1	Viking Lander 1
VL2	Viking Lander 2

Contents

List of publications

This thesis consists of an introductory review, followed by five research articles. The papers are reproduced with the kind permission of the journals concerned.

I Savijärvi H., Määttänen A., Kauhanen J. and Harri A.-M., "Mars Pathfinder: New data and new model simulations", (2004), Quarterly Journal of the Royal Meteorological Society, 130: 669–683.

II Määttänen A. and Savijärvi H., "Sensitivity tests with a one-dimensional boundary-layer Mars model", (2004), Boundary-Layer Meteorology, 113: 305–320.

III Määttänen A., Vehkamäki H., Lauri A., Merikallio S., Kauhanen J., Savijärvi H. and Kulmala M., "Nucleation studies in the Martian atmosphere", (2005), Journal of Geophysical Research, 110: E02002.

IV Vehkamäki H., Määttänen A., Lauri A., Napari I. and Kulmala M., "Technical note: The heterogeneous Zeldovich factor", (2007), Atmospheric Chemistry and Physics, 7: 309–313.

V Määttänen A., Vehkamäki H., Lauri A., Napari I. and Kulmala M., "Two-component nucleation kinetics and an application to Mars", (2007) Journal of Chemical Physics, 127: 134710.

1 Introduction

Mars and the Earth are neighbours in the Solar System. A fundamental need to explore our surroundings, typical for mankind, is the source of the interest driving us to space. Landers and orbiters have been sent to the red planet for decades, and modeling efforts have been of growing importance in designing the missions. Instrumentation, entry, descent and landing system design, landing site selection and aerobraking calculations need exact information on the Martian atmosphere, provided by observations and modeling studies. In particular, to have success on manned mission to Mars, we need to understand the Martian environment to which the astronauts would be exposed.

Terrestrial weather predictions are still far from perfect: research of planetary atmospheres can contribute to this via model testing and development of parameterizations. Terrestrial research of climate change is still puzzled by the role of aerosol particles in the process: they have an effect in the climate via influencing the radiative transfer. Increase in cloud occurrence increases the global albedo, thus cooling the planet, but clouds can also have a warming effect. Other aerosol particles can help in cloud formation, and they themselves scatter and absorb radiation. Mars has a family of aerosol particles in its atmosphere influencing the climate. The planet has been experiencing global change in the past, and may be experiencing it presently (Fanale et al., 1992; Kieffer and Zent, 1992; Fenton et al., 2007). Studies of climate variations on another planet can help us better understand our own global change.

Planetary research is thus a mixture of natural interest of the human imagination, and fundamental science, providing scientists with a very intriguing playfield.

The Martian atmosphere has been studied for decades both with observations and modeling, and already before the space age the mankind has pointed telescopes and eyes towards the red planet. First Mars missions in 1960-70's revealed an arid desert planet and created the foundation to our knowledge on Mars. After the Vikings in 1970's two decades passed without succesful missions to Mars, but during the last 10 years new missions have significantly increased the amount of observational data at hand. Future missions will hopefully answer questions still unresolved. In the light of present literature and the research I have done during my thesis I list here some of the outstanding questions that remain to be answered:

- What is the role and amount of subsurface water in the present climatic cycle of H_2O on Mars?
- What has caused the geologic features that seem as carved by flowing water?
- Was the atmosphere of Mars thicker and warmer in the past, and if so, what caused the thinning of the atmosphere?

- What is the process leading to the initiation of the quasi-regular global dust storms of Mars? What processes lead to global dust storms, and why some storms never expand outside local scale?
- What is the size distribution of dust and is it well-mixed in the atmosphere?
- What is the role of H_2O clouds in the hemispheric dichotomy of the global water cycle?
- How do CO_2 clouds form in the Martian atmosphere, particularly those at high altitudes? What has been their influence in the past climates of Mars?
- Do the two dominant volatiles always condense separately or do they form mixtures, such as clathrate or other types?

This thesis and the questions addressed in **Papers I–V** have implications to several of the aforementioned questions. Water cycle modeling near the surface compared with observations is important for understanding the role of the surface material and water fluxes from/to the atmosphere (Zent et al., 1993; Böttger et al., 2005) both in the present epoch and in studies of past geologic eras. The boundary layer processes are important for lifting of dust via saltation, thus demanding accurate boundary layer modeling (see, e.g., Siili et al., 1997). Particle formation studies address the first step in cloud formation. Correct cloud climatologies and thus correct prediction of cloud formation onset are important in studying the effect of clouds in the global cycle of volatiles. In particular, the role of cloud formation in the rising branch of the Hadley cell in limiting water vapor in the other hemisphere has been discussed (Clancy et al., 1996). The Martian atmosphere exhibits a rare phenomenon of condensation in near-pure vapour when CO_2 condenses on the polar ice caps and as clouds in the atmosphere: the release of latent heat in this process requires re-evaluation and thorough testing of the used theories. These processes also take place in a much more rarefied gas than on Earth, since the surface pressure of Mars is less than one percent of the surface pressure on the Earth. The role of CO_2 clouds in Martian paleoclimates (Forget and Pierrehumbert, 1997) has also been a topic in the discussion of the greenhouse effect in a thicker CO_2 atmosphere (Kasting, 1991; Colaprete and Toon, 2003). The thicker, warmer atmosphere may have enabled liquid water to flow on the surface, which could explain some geologic features we see on the surface of the planet. A thermodynamic analysis of the CO_2–H_2O -system suggests that condensation could happen also via other mechanisms than pure CO_2 or H_2O ice formation (Longhi, 2006). Laboratory experiments show possibilities for infrared detection of different mixtures of CO_2 and H_2O ices, implying that the ice mixtures could be detected also with orbiting infrared instruments (Schmitt et al., 2003; Galvéz et al., 2007). The composition of the polar ice caps still raises questions even with the very precise data and models we have at hand, showing room for improvement in our understanding of ice layering, ice mixtures and

condensation in the Martian conditions at present and in earlier epochs (Bibring et al., 2004a; Langevin et al., 2005; Douté et al., 2007; Levrard et al., 2007; Montmessin et al., 2007b). Theoretical particle formation modeling of the two components separately and together may shed light on condensation of ice mixtures, not only on the ground but also in the atmosphere.

Specifically, this thesis has the following main objectives:

- Look into the Martian boundary layer, understand the differences compared to the terrestrial boundary layer, and test parameterizations of a 1-D model against observations from Mars,
- discuss the roles of dust and water vapour in affecting radiative transfer in the atmosphere,
- take a closer look on ice crystal formation in the Martian atmosphere via models based on classical nucleation theory,
- develop the theoretical framework when needed,
- apply classical nucleation theory for multicomponent nucleation in Martian conditions for the first time and interpret the results,
- provide a link between aerosol and atmospheric studies in the Martian context, and
- lay a foundation for future prospects of research.

This thesis in structured in the following sections: in Section 2 I will give an introduction to the main features of Mars as a planet, and briefly summarize the history and present of observational missions to Mars, as well as some interesting future missions. I will introduce the Martian atmosphere and surface characteristics of the planet significant for atmospheric circulations. I will as well review the main topics of this thesis, the planetary boundary layer and clouds. In Section 3 I will briefly introduce the theories describing the planetary boundary layer, and I will summarize the studies of the included **Papers I–II**. Section 4 drills into the process of nucleation and describes the theoretical background governing new particle formation in a vapour. Section 4 also discusses the results of **Papers III-V**. Section 5 provides a link between boundary layer and nucleation studies as well as discusses the nature of different types of models, their significance, and drawbacks. Section 7 summarizes the main results of the thesis and opens views to the future.

2 Mars – the fourth rock from the Sun

2.1 Overview

Mars is a near neighbour to the Earth in the Solar System, and perhaps this is one of the reasons why Mars has always intrigued humans. Mars can be seen periodically as a fairly bright stellar object with a distinct red colour conceivable also with the naked eye. The colour may be the reason for the belief of Mars being the planet of war bringing bloodshed. Now we know that the colour is produced by oxidized iron-containing minerals of the Martian soil, and widespread suspended dust in the atmosphere, but nevertheless the bloodred colour may seize you while looking at the night sky.

Table 1: Comparison of astronomical parameters of Mars and Earth, adapted from Pellinen and Raudsepp (2000). The Astronomical Unit (AU) is a measure of the average distance of the Earth from the Sun.

Parameter	Mars	Earth
Mean distance from the Sun (AU)	1.52	1.0
Orbit eccentricity	0.093	0.017
Length of year (orbital period, Earth days)	687	365
Length of day (rotation period, Earth hours)	24.6	24.0
Obliquity (inclination of the rotational axis, °)	25.2	23.5

Mars is in some ways very similar to our planet, the Earth. At the present epoch the obliquities of Mars and the Earth are almost equal, and the rotational periods of the two planets (terrestrial day and Martian "sol") nearly coincide (see Tables 1 and 2). Thus the planets experience relatively similar seasonal and daily cycles, which is seen also in the resemblance of atmospheric motions and phenomena. However, Mars is further away from the Sun than the Earth, and thus also its year (the time it spends for making one round around the Sun) is longer, almost twice that of the Earth. The Martian seasons are often described with the help of L_s, the areocentric longitude of the Sun, which is defined as the angle between the line of equinoxes and the line from Mars to the Sun. This indicates that for the Martian spring equinox $L_s = 0°$, for the summer solstice $L_s = 90°$, for the autumn equinox $L_s = 180°$, and for the winter solstice $L_s = 270°$. The perihelion of Mars (the nearest point to the Sun on the orbit) occurs at around $L_s = 250°$, and the aphelion (the farthest point from the Sun) at $L_s = 70°$. At the perihelion the solar insolation at the top of the atmosphere (the solar constant) is about 35% larger than in the aphelion (709 W/m^2 compared to 499 W/m^2) because of the high eccentricity of the orbit. Thus the summer in the southern hemisphere is shorter and warmer, compared to the the northern longer but

cooler summer. The southern midsummer occurs near the perihelion, which is the most favorable time for the strongest and most widespread dust storms because of vigorous atmospheric circulation caused by the intense heating by the strong solar insolation.

Table 2: Comparison of planetary parameters of Mars and Earth, modified from Pellinen and Raudsepp (2000).

Parameter	Mars	Earth
Radius (Earth radii)	0.53	1.0 (=6378 km)
Gravitational constant at equator (m/s^2)	3.73	9.78
Average density (g/cm^3)	3.95	5.52
Mass (Earth mass)	0.1074	1.0 (=$5.976 \cdot 10^{24}$ kg)

The formation of the planet and its atmosphere, past climates, and geologic features are not included in this introduction, since they are out of the scope of this thesis. An extensive, general description of Mars as a planet can be found in Kieffer et al. (1992) and a summary of the features of the Martian atmosphere and climate in Read and Lewis (2004). The present knowledge of Mars in the light of new observations is published in the scientific literature (See Section 2.2.2 and references therein).

2.2 Observations

Scientific research in almost any field can be thought of consisting of three parts: observations and theory, which are combined by modeling. Theoretical studies are basic research that builds the foundation upon which our understanding of the world lies. Observations are a fundamental element of research, since they independently produce data on the true state of the studied target. Models function to establish a link between theory and reality. Observational data are needed for input for the models as well as for comparison with the output. Modeling community can not extend its research far with no observations at hand. Without observations modeling studies are reduced to interesting theoretical speculations, which, however, can be very significant in giving a first look into some previously unstudied topic and setting a basis for future studies (as in **Paper V**). In this section I will briefly go through the observational history of Mars and its implications for the work in this thesis. This is not, however, a complete review of observations of Mars. A good review of spacecraft exploration and telescopic observations of Mars before the 1990's is presented in Snyder and Moroz (1992) and Martin et al. (1992).

2.2.1 History

Telescopic observations of Mars have been conducted since the invention of the telescope in the 17th century, and surely the planet had been observed with the naked eye since the beginning of the history of mankind. The early telescopic observations revealed the growth and retreat of the polar caps, and changes in the brightness of the surface were seen. These features were linked also to possible vegetation on the planet, and a bit later in time, to canals.

Mariner space probes were planned to study the inner solar system, Mars and Venus in particular. Mariners 3 and 8 failed to reach Mars, but Mariners 4 (1964), 6 (1969) and 7 (1969) were the first successful spacecraft conducting observations during successful flybys of the planet. They revealed a dry, cratered, desert-like planet with a cold and thin CO_2 atmosphere. Mariner 9 mapped the planet for about 350 days from orbit starting November 1971, accompanied by Mars 2 and 3. The observations of the Mariners remained as the most complete basis for our knowledge on Mars for decades. See Snyder and Moroz (1992) for more details.

The Viking Orbiters (VO1 and VO2), with their respective Viking Lander companions (VL1 and VL2), arrived at Mars in 1976 and produced the first long data series of the planet. The VOs functioned for one (VO2) and two (VO1) Martian years, and the VLs transmitted over 3 (VL1) and 2 (VL2) Martian years of data from the surface. The VOs surveyed the atmosphere and the surface of the planet from above: they observed, for example, dust conditions, clouds, and polar ice caps (see, for example, Briggs et al., 1977). The main objective of the VLs was the discovery of life. In addition to the search of life the VLs made long-term meteorological observations of pressure, wind, and temperature. Both VO1 and VL1 observed early morning frost on the Martian ground (Briggs et al., 1977; Pollack et al., 1977). The morning fog observed by VL1 (Pollack et al., 1977) has been modeled by, for example, Savijärvi (1991b, 1995), and the morning fog observed by VO1 (Briggs et al., 1977) has been modeled by Inada (2002), and **Paper III** of this thesis. The VLs observed regular, daily scale changes in the pressure and winds, and these have been related to baroclinic low pressure systems that passed the landers at some distance (Tillman et al., 1979), which was seen also from VO1 (Hunt and James, 1979). Also the annual surface pressure cycle was measured well by the landers. The VOs observed the regular occurrence of so-called bore waves and long clouds, which seemingly were related to the interaction of slope winds in areas of large topographic variations (Hunt et al., 1981; Pickersgill and Hunt, 1981; Kahn and Gierasch, 1982). The VLs also observed the occurrence of the great global dust storms (Ryan and Henry, 1979). The VL datasets were processed with several calibration procedures, which cause the jumps seen in the data archived in the Planetary Data System. Also, parts of the data were recalibrated for publications. Thus no consistent analysis of the full dataset with the same algorithm and calibration has been performed yet. Now the full, original binary VL data (with the exception

of a few missing tapes), including the image, engineering, and meteorological data are waiting for new processing and reanalysis at the Finnish Meteorological Institute.

After the great success of the Viking mission, two decades passed without succesful missions to Mars. In 1997, however, two new missions finally reached its target and started observing the red planet. A lander, Mars Pathfinder (MPF), with the Sojourner rover arrived on Mars (Golombek et al., 1999). MPF Atmospheric Structure Investigation (ASI) accelerometer data provided data of the vertical structure of the atmoshpere between altitudes 161-8.9 km (Magalhaes et al., 1999), and it observed CO_2 supersaturation in the Martian atmosphere directly for the first time. MPF was equipped with a meteorological instrument package (Schofield et al., 1997) and it acquired 83 sols of data. MPF carried three temperature sensors at altitudes of 0.25, 0.50 and 1.0 m above the solar panels (approximately 0.52, 0.77 and 1.27 m above the ground). MPF also observed Martian clouds, water vapour, and the optical depth of the atmosphere with its camera that was designed especially for geologic observations (Smith et al., 1997; Smith and Lemmon, 1999; Titov et al., 1999). Also the orbiter Mars Global Surveyor (MGS) entered orbit and started observing the planet in 1997. The MGS functioned for almost ten Earth years, since the last transmission was received in November 2006. The datasets of the Thermal Emission Spectrometer (TES) of MGS on water vapour, dust optical depth and surface properties (Jakosky et al., 2000; Mellon et al., 2000; Christensen et al., 2001; Smith et al., 2001b,c, 2003), and the topography data of Mars Orbiter Laser Altimeter (MOLA) (Smith et al., 2001a) are the most important sources of input data for atmospheric models as of now. TES observations have also been used to recognize interannual variability in the Martian atmosphere (Smith, 2004).

Several probes were also lost, including the Mars Observer, Mars Polar Lander, Mars Climate Orbiter and the first European Mars lander, Beagle 2. The details of these probes will not be covered here.

2.2.2 Present

At the present moment the space around Mars is crowded, since there are three functioning orbiters (they were four before the loss of MGS in November 2006) observing the planet: 2001 Mars Odyssey (MOd), Mars Reconnaissance Orbiter (MRO), and Mars Express (MEx).

MEx is the first European Mars mission, and it has a comprehensive set of instruments onboard. It entered orbit in December 2003, has been operating well throughout its nearly four years in space, and continues in extended mission at least until end of October 2007. Atmospherically most significant instruments of MEx include PFS (Planetary Fourier Spectrometer, Formisano et al., 2005), OMEGA (Observatoire pour la Minéralogie, de l'Eau, des Glaces et de l'Activité, Bibring et al., 2004b), SPICAM

(SPectroscopy for Investigation of Characteristics of the Atmosphere of Mars, Bertaux et al., 2000), and HRSC (High Resolution Stereo Camera, Neukum et al., 2004; McCord et al., 2007). PFS is determining the composition of the Martian atmosphere, including trace gases such as CO and water. It can also measure the pressure and temperature profiles of the atmosphere. OMEGA was designed mainly to map the mineralogy of the surface, and it is the first near-infrared spectrometer in orbit of Mars. OMEGA is able to distinguish H_2O and CO_2 ice and determine the grain size of the ices (see, e.g. Langevin et al., 2005; Douté et al., 2007). OMEGA observations can also be used to study the atmosphere, and for example map the water vapour content (Melchiorri et al., 2007) or other trace gases, such as CO (Encrenaz et al., 2006), measure the surface pressure (Forget et al., 2007; Spiga et al., 2007), and observe atmospheric waves (Melchiorri et al., 2005). OMEGA can also detect dust suspended in the atmosphere (Garcia-Comas et al., 2006; Määttänen et al., 2006). SPICAM has been performing occultation measurements of atmospheric profiles (Montmessin et al., 2006c) and it has, for example, revealed the existence of high-altitude clouds (Montmessin et al., 2006a) and measured the concentration of ozone in the Martian atmosphere (Perrier et al., 2006; Lebonnois et al., 2006).

The following descriptions of the present NASA missions are mostly based on the World Wide Web pages of NASA (http://www.nasa.gov) for most up-to-date information, unless implied otherwise. The objectives of NASA's Mars Exploration Programme are to conduct extensive climate and geological studies, to look for signs of water and possibilities for past life, and prepare for human exploration. These are also the objectives of the two NASA orbiters, MOd and MRO. MOd was launched already in 2001, and is on its second extended mission. The instruments onboard include THEMIS (Thermal Emission Imaging System), which is similar to the TES of MGS, and has continued the mapping started by TES. MOd is functioning also as a linking station between the Earth and the MER rovers. The Gamma Ray Spectrometer (GRS) instrument has given first observational evidence of subsurface ice on Mars (Boynton et al., 2002). MRO (Zurek and Smrekar, 2007) is the newcomer in the fleet, and it started its primary observing phase in November 2006. Data from its instruments, for example MCS (Mars Climate Sounder, Taylor et al., 2005; McCleese et al., 2007), CRISM (Compact Reconnaissance Imaging Spectrometer for Mars, Murchie et al., 2007) and HiRISE (High Resolution Imaging Science Experiment, McEwen et al., 2007) are expected to give an image of Mars with unprecedentedly high resolution.

The Mars Exploration Rovers Spirit and Opportunity landed on Mars in January 2004, and measured atmospheric profiles on their way down (Withers and Smith, 2006). The rovers have functioned longer than ever expected: Spirit approximately 1340 sols and Opportunity 1280 sols by the mid-October 2007. During this time they had covered distances of 7.2 km (Spirit) and 11.5 km (Opportunity). Their main purpose has been the study of geology of Mars and mineralogy of the Martian surface materials. Thus the MERs do not have meteorological instruments onboard, but they carry a mini-

TES, which can be used to measure atmospheric temperature profiles. Both rovers have nine cameras, of which the Pancam can do multispectral observations with its set of filters, and the cameras can be used, for example, to derive the optical thickness of the atmosphere (Lemmon et al., 2004). The vertical temperature profiles of the rovers are a very useful tool for studying the Martian PBL (Smith et al., 2004), and they have been used already in comparison to PBL model results (Savijärvi, 2007). The mineralogical measurements of the surface may be able to tell us something about the composition of Martian dust, since the surface is the source of the dust. The rovers also study magnetic minerals and determine the fraction of magnetic versus non-magnetic particles in airborne dust and the material of the surface.

2.2.3 Future

The near-future missions in planning or implementation phase are the Phoenix Lander, Mars Science Laboratory, and ExoMars. Here only brief overviews of the missions are given, particularly in possible relevance to the work presented in this thesis.

The Phoenix Lander was launched 4th August 2007 and is set to land on an arctic plain of Mars in May 2008. It will carry, among others, a set of meteorological instruments including temperature and pressure sensor, and a LIDAR (LIght Detection And Ranging instrument) (Tamppari, 2006). It will also be able to monitor relative humidity with the help of its Thermal and Electrical Conductivity probe (Wood et al., 2006): this will be the first humidity sensor to have reached the surface of Mars. The objectives are similar to those of the present MOd and MRO orbiters, but Phoenix will specifically try to solve the question of subsurface water ice on Mars. At the landing latitude subsurface water ice should reside very near the surface, and the lander should be able to dig it out with the help of its robotic arm. The LIDAR will be able to detect dust and ice particles in the atmosphere and estimate their sizes, as well as measure the boundary layer height. The gas analyzer onboard will be able to reveal the composition of studied particles, in the best case also atmospheric dust.

Mars Science Laboratory continues the work of the MER rovers but in a greater scale, since it will be twice as long and three times as heavy as the MERs, and will also operate using a radioactive power source thus having more freedom to explore all seasons and locations desired. The launch is planned in 2009, and the lander will also host a meteorological instrument package (Vasquez and Gomez-Elvira, 2006) that will produce data on the state of the Martian PBL.

The ExoMars mission of the European Space Agency is planned to launch in 2013 an orbiter that will deliver a highly sophisticated lander on the surface of Mars. It will be searching for life, monitoring the chemical environment, and preparing for future manned missions via mapping possible hazards in the Martian environment.

Also networks of small landers have been planned for a long time, for example in the NetLander project (Harri et al., 1999; Polkko et al., 2000). The MetNet project (Harri et al., 2003) is actively pursued at the moment. Such a network of small meteorological stations on the surface of the planet would produce an unprecedented dataset of simultaneous observations from different locations giving a new view into the atmospheric near-surface phenomena. An observational network is also a prerequisite for weather forecasting. The European Space Agency also has frameworks for future network missions (ExoMars and NEXT).

2.3 The Martian atmosphere

The atmosphere of Mars exhibits very similar phenomena as the atmosphere of the Earth. Our current understanding of the atmospheric processes is good, but several outstanding questions remain, related to, for example, the initiation and quasi-periodicity of the dust storms, the balance of the Martian water cycle, the dichotomy of the two polar caps, connection between the subsurface and the atmosphere, and the formation mechanism of high-altitude CO_2 clouds. Our knowledge is based on modeling efforts and observations made by a fleet of orbiters and landers that have probed the planet since the early years of space flight (See Section 2.2).

Mars has a thin and cold CO_2 atmosphere that also includes small amounts of nitrogen, argon, oxygen, ozone and other trace gases, and also some water (see Table 3). The most important volatiles are CO_2 and H_2O, and they can be found in either vapour or solid phase in the present atmospheric pressure and temperature ranges. However, in some locations on the surface it may be possible to reach a state where liquid water could exist (Haberle et al., 2001; Hecht, 2002), but for the atmospheric processes the liquid state can be overlooked. The uneven distribution of solar insolation on the planet causes a temperature gradient between the equator and the poles, thus giving rise to atmospheric general circulation, which exhibits large Hadley-cells, one or two depending on the season. The surface of Mars responds to heating strongly, and functions as the driver of atmospheric motions, but also gaseous and dust absorption of solar and thermal radiation in the atmosphere have an influence on the circulation phenomena. The diurnal and semidiurnal thermal tides are very strong in the dusty atmosphere of Mars, and the autumn and winter midlatitudes experience baroclinic instability giving rise to low pressure systems around the winter pole. On the local scale the Martian topography (with elevation scale of more than 30 km) drives mesoscale circulation phenomena, such as slope winds and sea breeze -type circulations caused by differential heating of the surface in adjacent areas. The circulations also induce cloud formation, for example, via adiabatic cooling in updrafts of slope winds, in the ascending branch of the Hadley cell, in large-scale rising motion of low pressure systems, and radiative cooling of the surface layer during the night (radiative fogs). Good summaries of

the aspects of the general circulation, waves, tides, and other significant atmospheric phenomena can be found in Zurek et al. (1992) and in Read and Lewis (2004).

Table 3: Composition of the Martian atmosphere (in % for the six major substances and in parts per million, ppm, for the minor ones) from Owen (1992).

Gas	Symbol	Proportion
Carbon dioxide	CO_2	95.32 (%)
Nitrogen	N_2	2.7
Argon	^{40}Ar	1.6
Oxygen	O_2	0.13
Carbon monoxide	CO	0.07
Water vapour	H_2O	0.03
Argon	$^{36+38}Ar$	5.3 (ppm)
Neon	Ne	2.5
Krypton	Kr	0.3
Xenon	Xe	0.08
Ozone	O_3	0.04–0.2

One of the peculiarities of Mars is that approximately a quarter of the atmosphere itself condenses on the winter pole. CO_2, the major component in the atmosphere, takes part in condensation, and forms the polar ice caps along with water ice. The CO_2 condensation on the autumn/winter pole and sublimation from the spring/summer pole causes a distinct annual oscillation in the average surface pressure, p_s, of Mars, and locally the oscillations can be as large as 25–30% (Tillman, 1988; Tillman et al., 1993). The sublimation and condensation between poles is not only seen in the surface pressure oscillation, but also as a sublimation/condensation flow from summer pole to winter pole. The surface temperature, T_s, is limited because of CO_2 condensation: if the temperature decreases enough for CO_2 to start condensing, the decline of temperature stops because of the latent heat release. Since for Mars the partial pressure of CO_2 nearly equals the local pressure (95.3% CO_2 atmosphere), a good approximation for the condensation temperature on the surface is defined by the local surface pressure (the partial pressure of the CO_2 vapor). Also CO_2 clouds form in the atmosphere, particularly in the polar winter night (Ivanov and Muhleman, 2001; Pettengill and Ford, 2000; Colaprete and Toon, 2002; Colaprete et al., 2003; Tobie et al., 2003), but also high altitudes in the atmosphere elsewhere on the planet (James et al., 1992; Clancy and Sandor, 1998; Montmessin et al., 2006a,b, 2007a). Martian clouds will be reviewed more in detail in Section 2.6.

For water vapour the condensation temperature can not be defined in an equally simple manner as for CO_2. The amount (and thus partial pressure) of water is very variable in the Martian atmosphere and depends on location and on the season and time of day.

Water ice is found not only in clouds and fogs in the atmosphere (see Section 2.6), but a major part of it resides in the polar ice caps. The permanent ice cap on the north pole is mostly water ice, onto which a layer of seasonal CO_2 ice forms during autumn and winter only to sublime away in the spring. During summertime the water ice cap persists in the north. The vapour amount in the atmosphere is often described with the help of precipitable water amount: this is the thickness of a layer of water if all the water from an atmospheric column would be condenced on the surface. On Mars this in the range of micrometers, when on the Earth it is of centimeter scale. The water cycle on Mars is asymmetric exhibiting largest atmospheric water vapour amounts (up to 70–100 μm) near the edge of the northern ice cap in the summer after the seasonal CO_2 frost cap has sublimed and exposed the water ice (Jakosky and Farmer, 1982; Smith et al., 2001b; Smith, 2002). A similar, but smaller (40 μm), maximum is observed near the southern polar ice cap edge during the respective summer (Smith et al., 2001b; Smith, 2002). Because of the variability of water vapour concentration, the temperature where saturated state is reached depends a lot on time and location, and can not be directly linked to any one variable like in the case of CO_2. The condensation temperature depends on the partial pressure of the vapour and the temperature of the ambient air, and needs to be calculated for all conditions separately. This topic, related to cloud formation, will be covered in detail in Section 4.

The dust cycle is under intensive research, and observations, dating from long ago show that large, global or hemispheric, dust storms occur quasi-periodically with a preference for the summer of the southern hemisphere. For summary of observations since the 19th century see, for example Martin and Zurek (1993) and Jakosky (1995), and for the latest most complete datasets see Smith et al. (2001b,c) and Smith et al. (2003). Annual occurrence of dust storms has been studied by Cantor et al. (2001) for the year 1999 dataset of Mars Orbiter Camera observations. As mentioned earlier, the southern hemisphere summer is the period of the maximum solar insolation, which also implies more vigorous dynamics of the atmosphere. However, regional or local scale dust storms occur at all seasons (see, e.g. Cantor et al., 2001). The dust is lifted to the atmosphere by a process called saltation, which requires wind speeds high enough to be able to lift and move small sand grains, which kick off small dust particles when hitting the ground again. To attain the treshold of saltation, small-scale phenomena with high wind speeds, like dust devils, are most probably needed, since the background wind speeds may not be enough. Dust devils are common on Mars according to observations (Thomas and Gierasch, 1985; Metzger et al., 1999). Their spatial scale exceeds that of their terrestrial siblings, and they are able to lift dust from the surface, also shown by modeling (Kanak, 2006; Kurgansky, 2006; Michaels, 2006), and theoretical evaluations (Renno et al., 2000). Greeley (2002) studied the process of saltation dust lifting experimentally and Greeley et al. (2003) performed experimental studies of dust devil formation and particle lifting in them. After saltation, the small dust particles are further mixed into the atmosphere by atmospheric circulation. During global dust storms a veil of dust mixed through the atmosphere can cover the whole

planet. The properties of Martian dust have been evaluated by, e.g., Pollack et al. (1979); Ockert-Bell et al. (1997); Forget (1998); Tomasko et al. (1999); Fedorova et al. (2002); Clancy et al. (2003) and Wolff and Clancy (2003), and the Martian dust cycle has been modeled by, e.g., Murphy et al. (1995); Newman et al. (2002a,b), and Basu et al. (2006). Basu et al. (2006) presented the first modeling of spontaneous dust storm development with realistic interannual variability in a global general circulation model of Mars, whereas previous models have had to either be forced to observations (in lack of dust lifting mechanisms) or have not presented enough interannual variability.

Thus the major climatic cycles in the atmosphere are the global cycles of CO_2, water, and dust. The connection between the aforementioned cycles is cloud formation, which is also the second major topic of this thesis. CO_2 and water ice clouds form on dust particles via heterogeneous nucleation and consequent condensation. This link, its strength and coverage has a strong impact on the climate, both present and past, and is one of the key points when trying to understand the present climatic system of Mars. The connection between ice cloud formation, dust and water redistribution and atmospheric radiative transfer and temperatures is very nonlinear and requires accurate description of the processes involved. The process of cloud formation will be covered in detail in Section 4.

2.4 The surface of Mars

The topography of Mars and its large variations have been mapped very precisely by the Mars Orbiter Laser Altimeter (MOLA) onboard the Mars Global Surveyor (MGS) (Smith et al., 2001a). Also the OMEGA instrument onboard Mars Express (Bibring et al., 2004b) is able to map parts of the surface with very high horizontal resolution (Melchiorri et al., 2006). These data provide us knowledge on the Martian surface and its variations with high accuracy. The topography variations are large, covering more than 30 km from the bottom of Hellas basin (-9 km from the reference surface, where the annual mean pressure is the triple point pressure of water, 6.11 hPa) up to the top of Olympus Mons (+27 km). Other outstanding features are the impact basin of Argyre and the chasms of Valles Marineris. The northern hemisphere is very flat and low, and resembles greatly the bottom of an ocean. The southern hemisphere is much higher than the northern, thus causing a topographical dichotomy that has an effect on the atmosphere as well.

However, the elevation is not the only property of the surface. Other significant properties of the surface are the albedo and thermal inertia. These properties were already mapped by Viking Orbiters (Kieffer et al., 1976, 1977), and more recently by the TES instrument on MGS (e.g., Mellon et al., 2000; Christensen et al., 2001), and by THEMIS onboard Mars Odyssey (Fergason et al., 2006). The albedo is the ratio of reflected and incoming solar radiation, so it gives the fraction of solar flux that is reflected away (the

rest is absorbed by the surface). The thermal inertia I is a variable that describes the ability of a material to resist the effect of changes in insolation that can be seen as the time lag between the change in insolation and the reaction of the material. The higher the thermal inertia is, the less the material reacts to insolation: the amplitude of temperature variations is smaller and the reaction is slow. Good examples of high thermal inertia are the oceans (liquid water) and ice. A material with small thermal inertia reacts fast and the amplitude of the variation is higher. These features are looked into in more detail in Section 3.

Because the atmosphere of Mars is very thin, and thus the turbulent heat fluxes from the surface small, the thermal balance of the surface is controlled by radiation. This is also the reason for very large observed temperature gradients between the surface and the lowest layers of the atmosphere: 10–15 K at Mars Pathfinder landing site (Schofield et al., 1997), and 30 K at some sites the Mars Exploration Rovers have covered (Smith et al., 2004). The properties and effects of the surface are important, since in general the circulation in the planetary boundary layer (PBL, see Section 3) is strongly controlled by the thermal properties of the surface. However, on Mars also the radiative heating/cooling of the atmosphere is essential in the PBL.

Two interesting locations having extreme features of the surface are the polar caps. The permanent polar ice caps are thick and rise significantly above their surroundings (Smith et al., 1999). These topographical features are prominent and give rise to atmospheric circulations (e.g., Ye et al., 1990; Siili et al., 1997, 1999). The albedo and thermal properties have a large gradient just at the edge of the ice caps: ice reflects more solar radiation than the regolith, and the thermal inertia of ice is also very high. The polar caps are during their respective winters covered by a seasonal, some meters thick layer of CO_2 ice. A permanent, kilometers thick ice cap of water remains in the north pole (see Langevin et al., 2005, for latest observations), and a thick, permanent CO_2 ice cap mixed with water ice (see Bibring et al., 2004a; Douté et al., 2007, for latest observations) remains in the southern summer pole. Thus the polar ice caps function as sources/sinks of the atmospheric volatiles, and are major components of the climatic cycles. They are also important for atmospheric circulations, both in local (ice edge circulations) and in global (sublimation/condensation flow) regime.

2.5 The planetary boundary layer

The planetary boundary layer is the layer of the atmosphere that is closest to the surface, and is characterized by the influence of surface heat fluxes and friction on the flow. The effect of friction is transported upwards by turbulent eddies. Simultaneously the eddies efficiently mix all other variables, e.g. temperature, humidity, trace gases, and aerosol particles. Turbulence is formed by the mechanical drag of the surface, and by thermal convection, forming when the surface heats up. Thus the overall effect

varies with location, local time, and season. Turbulence is still scientifically not well understood, and the theories describing it are, to large extent, based on (semi)empirical fits. One of the problems in describing turbulence is the so-called "closure problem". In order to calculate the first-order variables describing the turbulent fluxes (the turbulent variables in this case are the deviations of the variables from the average), also the second-order variables (being the deviations of the first-order deviations) are needed, and so forth. To solve this problem we are obliged to decide which order of "closure" to use. This will be described in Section 3.1

The processes of the Martian PBL have been studied via observations and modeling. The first landers on Mars, the Viking Landers 1 and 2 in the 1970's, transmitted more than three Martian years of meteorological data from two sites on the surface of Mars (Hess et al., 1976, 1977). The next lander arrived 20 years later, when Mars Pathfinder found its way down to collect meteorological data for 83 sols (Schofield et al., 1997). The latest surviving landers, the Mars Exploration Rovers (MERs) Spirit and Opportunity have, in the absence of meteorological equipment, produced image material on phenomena like dust devils, and also some measurements of the PBL thermal profile via their mini-TES instruments (Smith et al., 2004).

After the first data from the surface of Mars arrived, the theories, models, and empirical fits derived for the terrestrial boundary layer were also applied on Mars. Several studies were made using the data from Viking Landers 1 and 2, and 20 years later Mars Pathfinder produced a new dataset. The Viking Lander data was looked into by Seiff and Kirk (1977); Sutton et al. (1978) and Tillman et al. (1994) and modeled, for example, by Haberle and Houben (1991); Haberle et al. (1993); Savijärvi (1991b) and Savijärvi (1995). Haberle et al. (1997) made a weather prediction for the Mars Pathfinder lander, and after landing the MPF data were presented by Schofield et al. (1997), looked into by Larsen et al. (2002), and modeled, for example, by Savijärvi (1999) and **Papers I–II**. The aforementioned studies concluded that the similarity theory of turbulence derived in terrestrial conditions also applies well for Mars.

In the terrestrial PBL convection primarily transports heat from the surface warmed by the solar flux higher to the atmosphere. However, one peculiarity of the Martian PBL is that also radiative effects of CO_2 and dust in the atmosphere are very important. Actually, the longwave absorption of surface-emitted radiation by these substances in the atmosphere, the absorption of solar shortwave radiation by dust, and the consecutive longwave emission and heating of the surrounding air are so strong that convection acts as a cooling factor in the lowest layers of the PBL. In other words, even though the surface layer of the PBL is highly unstable and convective, convection acts (in contrast to terrestrial convection) to cool down the lowest layers of the atmosphere heated very strongly by longwave absorption of CO_2 and dust. Thus on Mars the daytime PBL is more radiatively driven than convection-driven. This is seen also in the model results of **Papers I–II**, an example of which is presented in Figure 1. The Figure 1 shows the heating rates due to turbulence in units K/h as a function of altitude. The heating

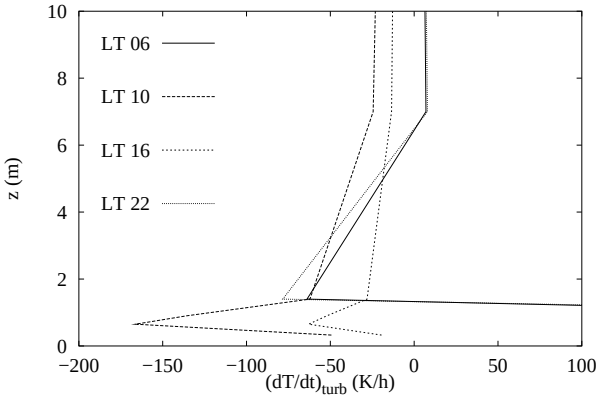

Figure 1: An example of a 1-D model result on the heating rate due to turbulence near the surface at different local times in Pathfinder conditions (season L_s=140°). The cooling effect of turbulence can be seen throughout the day below 7 m altitude. z is the altitude, T is temperature, t time, and $(dT/dt)_{\mathrm{turb}}$ is the heating rate due to turbulence (in units K/h).

rates are generally negative throughout the day below 7 m altitude, which means that convection is cooling the air at those altitudes. However, in cases with prevailing background wind, during the night the roles of radiation and convection are switched. A very stable inversion layer is established after the well-mixed convective daytime PBL rapidly dissipates after sunset. In the inversion layer the rapidly cooling surface and turbulence cool the atmosphere right above the surface, and radiative cooling is the major agent only higher up in the atmosphere.

The significant differences between the terrestrial and Martian PBLs that can be distinguished are the aforementioned roles of convection and radiation, the larger kinematic viscosity (smaller Reynolds number) and the height of the boundary layer, which in the more rarified Martian atmosphere can be tenfold higher (extending up to 10 km) compared to the Earth. The potential temperature is conserved in adiabatic processes, and is thus constant in a well-mixed PBL. In Figure 2 the boundary layer height (here the height of the mixed layer) is seen as a constant profile of the potential temperature θ. In the case of Fig. 2 the well-mixed layer grows up to 5 km during the day.

One interesting feature of the effect of turbulence on the flow is the formation of the nocturnal supergeostrophic nocturnal low-level jet. Normally the wind speeds in the PBL are lower than above it, where the so-called geostrophic assumption holds well for large-scale winds. In the case of a non-zero background geostrophic wind a nocturnal low-level jet can form in the following way: during the day the friction gives rise to an ageostrophic component of the wind (see Figure 3a), but when sun sets and convection stops, the surface and the atmosphere are decoupled (i.e. the effect of friction is switched off). The remaining ageostrophic component starts turning clock-

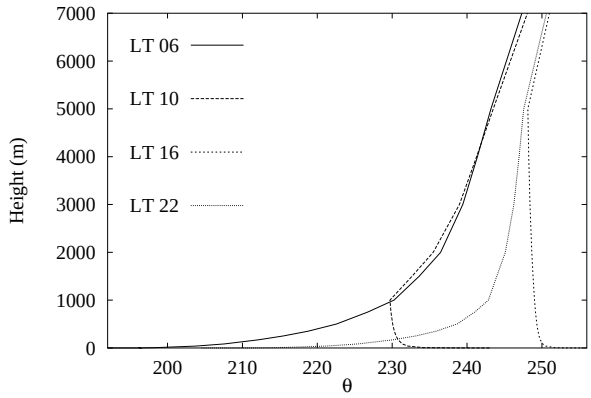

Figure 2: An example of the 1-D model-predicted potential temperatures (θ) with respect to height in Pathfinder conditions (season L_s=140°): the θ-profile can be used to describe the boundary layer height as the layer in which θ is constant (where the profile of θ is approximately vertical, as in local times LT 10 and LT 16).

wise in the northern hemisphere in inertial oscillation, and at some moment coincides with the geostrophic background wind component (see Figure 3b). At this stage the wind speed (the sum of the now parallel background geostrophic wind and the rotating ageostrophic component) reaches its maximum, and this supergeostrophic wind is called the nocturnal low-level jet. This phenomenon is strong when the ageostrophic component of the wind is large during the day (strong convective turbulence), the PBL collapses rapidly after sunset, the night is sufficiently long for the inertial oscillation to turn the wind enough, and the nighttime PBL is very stable (e.g., Haberle et al., 1993). It seems that the Martian PBL has favorable conditions to meet these requirements for the nocturnal low-level jet formation. The nocturnal low-level jet was observed at around 300 m altitude at 06 LT in the model results of **Papers I–II**.

The theory of turbulence in the boundary layer and the results of **Papers I–II** will be looked into in Section 3.

2.6 Clouds and fogs

Clouds are an important part of any climate. In the terrestrial climate change studies the effect of aerosol particles (including clouds) is still one of the biggest unknowns (Houghton et al., 2001; Solomon et al., 2007). In a possibly thicker ancient Martian atmosphere the radiative effects of clouds may have been significant possibly even enabling liquid water on the surface (Forget and Pierrehumbert, 1997). For accurate modeling of past climates, the present climate needs to be understood and adequately modeled. Thus cloud formation and their climatology is one of the key points in

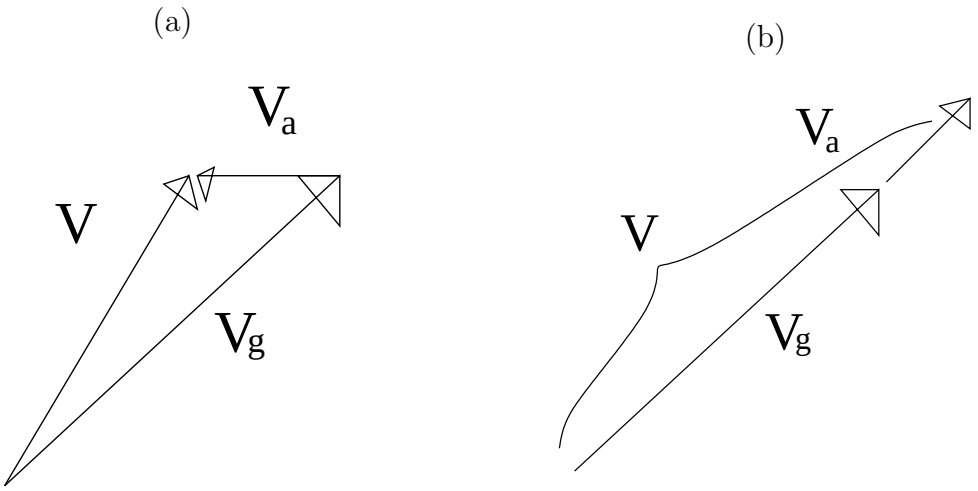

Figure 3: The formation of a nocturnal low-level jet: a) During the day the near-surface winds are a sum of the geostrophic background wind and the agestrophic component of the wind forming because of turbulence (friction), b)during the night the ageostrophic component oscillates clockwise and at some point coincides with the geostrophic wind direction. Thus this situation is called the supergeostrophic wind and a nocturnal low-level jet, because it happens in the boundary layer during the night.

Martian climate studies.

A review of knowledge on Martian cloud systems established by mid-80's (including water, CO_2 and dust clouds) can be found in Hunt and James (1985). The latest dataset has been acquired by MGS (the first year of observations is described in Pearl et al. (2001)).

The climatology of Martian water ice clouds, the major cloud type, exhibits clear seasonal patterns, of which the most prominent are the polar hoods that form around and over the autumn/winter pole, and the aphelion cloud belt that forms in the northern hemisphere summer in the ascending branch of the Hadley cell, (see, for example, Clancy et al., 1996; Wolff et al., 1999; Tamppari et al., 2000, 2003). A comprehensive cloud climatology study based on VO images made by Kahn (1984) is still waiting for a successor: the MGS/MOC has collected a vast dataset than can be utilised to focus our view on the climatology of water ice clouds on Mars. The MOC dataset has been used so far for studies of polar hoods and the tropical cloud belt (Wang and Ingersoll, 2002). Clouds do form also elsewhere than in the polar night and Hadley circulation, and some preferred locations are the slopes of the great volcanoes in the Tharsis area (see, for example, Pickersgill and Hunt, 1981; Zasova et al., 2005; Noe Dobrea and Bell, 2005; Michaels et al., 2006; Benson et al., 2006). Clouds are a major part of the water cycle and exhibit strong, nonlinear connection with the dust cycle and atmospheric temperatures. The water ice clouds act as scavengers of atmospheric dust, as do CO_2 ice clouds, since the large ice crystals fall out from the formation altitudes,

thus redistributing both dust particles and water in the atmosphere. This has been studied, e.g., by Michelangeli et al. (1993) and Rodin et al. (1999). Surface (radiative) fogs form during nighttime, especially in the morning hours, when longwave cooling is strong, and the surface and lowest layers of the atmosphere cool down to temperatures low enough for ice crystal formation to initiate. The properties of Martian water ice particles have been studied, e.g., by Clancy et al. (2003) and Wolff and Clancy (2003). They classified the clouds into two classes. Type 1 clouds are found in the southern hemisphere as well as in high-altitude and topographically-induced hazes, they indicate small particle effective radii of $r_{\text{eff}} = 1 - 2$ μm, and they exhibit clear increase towards backscattering in the phase function. Type 2 clouds are frequent in the aphelion cloud belt in the northern summer subtropics, exhibit larger particle size ($r_{\text{eff}} = 3 - 4$ μm) and show a minimum in the side-scattering part of the phase function. Montmessin et al. (2006c) discovered a cloud type 3 exhibiting significantly smaller particle sizes ($r_{\text{eff}} = 0.1$ μm) in clouds located at high altitudes, at 70–100 km, seen in SPICAM limb observations.

CO_2 clouds on the Martian limb were already observed by Mariner 6 and 7 (James et al., 1992; Clancy and Sandor, 1998), but the observations were for long overlooked since the observed clouds were thought to reside too low in the atmosphere for low enough temperatures for CO_2 condensation to occur. Thus CO_2 cloud formation was speculated to happen primarily in the polar night, where temperature can decrease enough to reach CO_2 saturation. The polar CO_2 clouds were observed indirectly by MOLA (Pettengill and Ford, 2000; Ivanov and Muhleman, 2001), and modeled by Colaprete and Toon (2002); Colaprete et al. (2003), and Tobie et al. (2003). The polar CO_2 clouds are speculated to be convective exhibiting so-called moist convection (related to immense latent heat release in condensation of near-pure vapour), and also snowfall (Colaprete and Toon, 2002; Colaprete et al., 2003; Tobie et al., 2003). CO_2 nucleation on dust particles requires high supersaturations (saturation ratio $S > 1.3$), and thus strong temperature deviations from (sub)saturated state. The formation of supersaturated state can be facilitated by gravity waves formed by flow over the very variable Martian topography, particularly in the southern polar areas (Colaprete and Toon, 2002; Colaprete et al., 2003; Tobie et al., 2003). After condensation begins, the released latent heat warms the air and promotes updraft, in a similar fashion as moist convection in terrestrial cumulonimbus clouds. So the CO_2 clouds are a very dynamical feature of the atmosphere, whereas water ice clouds, and surface fogs, are less vigorous in nature but more frequent in appearance, since water nucleates in higher and more prevailing temperatures than CO_2. Clancy and Sandor (1998) argued that the CO_2 ice signature seen by Mariner 6 and 7 was really created by clouds, and they also suggested that the blue clouds observed by the Mars Pathfinder were mesospheric CO_2 clouds. The latest observations by SPICAM and OMEGA on Mars Express have proven directly that CO_2 clouds also form very high in the atmosphere outside polar areas (Montmessin et al., 2006a,b, 2007a). Also MGS observed high-altitude clouds with its Thermal Emission Spectrometer and Mars Orbiting Camera, but did

not distinguish between water ice and CO_2 ice (Clancy et al., 2007). However, the observations of OMEGA, SPICAM, TES and MOC indicate that occurrence of CO_2 clouds on Mars is more widespread and not only limited to the polar areas.

According to our present knowledge the Martian cloud particles form on pre-existing surfaces of ubiquitous dust particles. The process of particle formation thus happens via heterogeneous nucleation, where thermodynamically stable clusters form on some pre-existing particle and then grow by condensation. It has been assumed in several studies (Glandorf et al., 2002; Colaprete and Toon, 2002, 2003; Colaprete et al., 2003; Tobie et al., 2003) that H_2O-coated dust particles function as the condensation nuclei for CO_2 crystals. And indeed, the study of Gooding (1986) has shown that water ice may be more efficient as CN for nucleating CO_2 than the Mars dust analog minerals used in his study. However, we have assumed pure dust particles throughout our studies for two reasons. First, there is very little data on the parameters (such as the contact angle) describing interaction between the CN surface and the nucleus for the Martian substances: thus our assumptions for the parameters do not necessarily describe well either of the cases (water ice coated dust or pure dust). Second, CO_2 cloud formation on Mars can happen in circumstances where water ice is absent: either the atmosphere is simply too dry, or water has been scavenged away by previous crystal formation and subsequent settling out. However, when performing modelling of clouds with a coupled cloud-atmosphere model, the possibility of water ice coated dust grains as CN should be accounted for. So far, only CO_2 and H_2O clouds have been detected in the Martian atmosphere, and the process of one-component nucleation of both components have been studied in **Papers III-IV**. Multicomponent and heterogeneous nucleation may have a significant role in particle formation in the terrestrial atmosphere (Kulmala et al., 2006), and it now seems that hydrate clathrates of CO_2 or eutectic mixtures of solid CO_2 and clathrate or water can condense on Mars (Longhi, 2006). According to Schmitt et al. (2003) CO_2 hydrate clathrate can possibly be observed in the polar areas of Mars. Laboratory experiments by Galvéz et al. (2007) provide constraints for measurable infrared spectra of different mixtures of CO_2 and H_2O ices, showing possibilities that the ice mixtures could be detected with orbiting high-resolution infrared instruments. **Paper V** presents the first modeling investigation of two-component nucleation on Mars.

I will describe the process of cloud formation in more detail in Section 4, where I will also summarize the results of nucleation modeling.

3 The planetary boundary layer on Mars

A description of the planetary boundary layer of Mars and a short summary of observations and modeling of the Martian PBL were given in Section 2.5. In the following I will briefly go through the basic theory of turbulence in the boundary layer, particularly the parts not covered by **Papers I–II**. The description of the basic theory here is roughly following the very concise summary presented in Savijärvi and Vihma (2001), but a thorough review of the theory of turbulence in the PBL can be found from, for example, Arya (1988) and Stull (1988). I will also introduce the model used in **Papers I–II**, and to conclude this chapter, I present briefly the main objectives and results of the related **Papers I–II**.

3.1 Theory of turbulence in the boundary layer

Mechanical turbulence is caused by the no-slip boundary condition at the surface, where the velocity goes to zero, forcing the fluid molecules to slide over each other. Flow becomes turbulent when the flow speed is high enough. The formation of turbulence in a flow depends on the velocity of the flow U, its length scale L and the kinematic viscosity of the fluid ν. A dimensionless number, the Reynolds number, describes the ratio of the inertial force of the flow to the internal friction of the flow. The Reynolds number is defined as $Re = UL/\nu$, and once it exceeds a certain critical value, the flow becomes turbulent. Turbulent flow exhibits large variances, the flow speeds vary and are gusty, properties of the fluid are mixed well by the turbulent eddies, and the flow is dissipative, so turbulence takes energy from the flow itself.

The Navier-Stokes equation is the Newton equation for a viscous fluid and reads (in vector form)

$$\frac{\partial \boldsymbol{V}}{\partial t} + (\boldsymbol{V} \cdot \nabla)\boldsymbol{V} = -\frac{1}{\rho}\nabla p + \nu \nabla^2 \boldsymbol{V} + \Sigma \boldsymbol{F_i}. \tag{1}$$

The terms of Eq. (1) are (from left to right): the tendency of velocity (temporal change of velocity in a fixed point), advection term, the pressure gradient force driving the circulation, molecular diffusion, and the sum of all other forces (e.g. Coriolis and gravity forces). $\boldsymbol{V}$ is the velocity vector, ρ is the three-dimensional density field of the fluid, and p is that of pressure. The variables in a turbulent flow can be described with the help of so-called Reynolds decomposition, where the value of the variable at some point in time is the sum of the time average of the variable (denoted by overbar) and a fluctuating part (denoted by prime): $c = \bar{c} + c'$. The prognostic equations for any variable c in the flow are of the form

$$\frac{Dc}{Dt} = \frac{\partial c}{\partial t} + \boldsymbol{V} \cdot \nabla c = S_c \tag{2}$$

where the first term on the right-hand side is the tendency and the second term the advection of the variable c. S_c represents the source/sink term for the variable. With the help of Reynolds decomposition, taking a time average, and a fair amount of manipulation we get

$$\frac{\partial \overline{c}}{\partial t} + \overline{\boldsymbol{V}} \cdot \nabla \overline{c} = \overline{S}_c - \nabla \cdot (\overline{c' \boldsymbol{V}'}). \tag{3}$$

The last term on the right-hand side of Eq. (3) is the turbulent flux convergence. It describes the net effect of turbulent mixing to the time variations of the average (tendency of $\overline{c}$, first term on the left-hand side of Eq. (3)). Normally the horizontal terms can be neglected since they are small (horizontally homogeneous turbulence) and only the convergence of the turbulent vertical flux remains. Thus the prognostic equation (neglecting advection) becomes

$$\frac{\partial \overline{c}}{\partial t} = \overline{S}_c - \frac{\partial (\overline{c'w'})}{\partial z}, \tag{4}$$

where w' is the fluctuation of the vertical wind component w, and the overbar denotes a time average. Now the turbulent vertical fluxes (last term on the right-hand side of Eq. (4)), which are large in the PBL, need to be described. This can be achieved in two ways: either they are described with the help of the averages of the variables (first-order closure), or by formulating new prognostic equations for them (higher-order closure). The latter alternative, however, will include turbulence terms of higher degree (involving variables of type $\overline{c''w''}$), which again have to be described in one of the aforementioned ways. This way the "closure problem" of turbulence is only postponed further in the higher-degree approach.

Most often first-order closure is used, meaning that the covariance terms are described with the help of vertical gradients of the means using a diffusion-type equation

$$\overline{c'w'} = -K_c \frac{\partial \overline{c}}{\partial z}. \tag{5}$$

The eddy viscosity coefficients (K_c) analogous to a diffusion coefficient can be evaluated using turbulence measurements, and it appears that the coefficients for scalars (temperature, humidity, and so forth) are equal, but they differ from that of momentum. Now, after substitution of (5) the prognostic equation, Eq. (4), becomes

$$\frac{\partial \overline{c}}{\partial t} = \overline{S}_c + \frac{\partial}{\partial z} \left(K_c \frac{\partial \overline{c}}{\partial z} \right). \tag{6}$$

The eddy coefficients need to be inside the derivative since they depend on the flow and its stability and thus vary strongly in time and space. Equations for the eddy viscosity coefficients will be described later.

The static stability could be described as a precursor of turbulence, and it is related to the temperature profile of the layer involved. Stability of the atmosphere can be

described, for example, with the help of a dimensionless Richardson number Ri, which is the ratio of the two components producing turbulence: buoyancy and shear. Buoyancy is related to density differences and thus temperature differences, and shear is the change in wind direction and/or change in wind velocity with height. Ri can be defined, for example, in terms of the vertical gradients of the variables, in which case it is called the gradient Richardson number:

$$Ri = \frac{\frac{g}{\theta}\frac{\partial \theta}{\partial z}}{\left(\frac{\partial u}{\partial z}\right)^2} \tag{7}$$

where the numerator is the component describing the effect of buoyancy, and the denominator the effect of the vertical wind shear.

Another useful measure is the friction velocity, which is connected to the turbulent momentum flux in the surface (constant-flux) layer. It is defined as $u_* = \sqrt{-\overline{u'w'}}$ and it is used in the following for defining the eddy viscosity coefficients. The sign convention here is such that flux from the atmosphere is negative, thus $\overline{u'w'}$ is negative since in the PBL the momentum flux is always towards the surface, and the minus sign is needed in the square root to end up with a nonimaginary result.

The eddy viscosity coefficients that appeared in Eq. (5) and Eq. (6) can be described in different ways: in a neutral flow the coefficient for momentum K_m is of the form

$$K_m = l^2 |\frac{\partial U}{\partial z}|, \tag{8}$$

where the mixing legth $l = kz$ describes the typical size of the eddies, and k is the von Karman's constant. A neutral flow is the simplest case, where the mean wind velocity profile depends only on altitude and the momentum flux (which is constant in the surface layer). The only possible non-dimensional combination of these variables determining turbulence gives

$$\frac{z}{u_*}\frac{\partial u}{\partial z} = \frac{1}{k}, \tag{9}$$

which can be integrated upwards from the altitude where the average wind velocity is zero (so called roughness length, z_0) to yield

$$u(z) = \frac{u_*}{k}\ln(\frac{z}{z_0}). \tag{10}$$

This is the famous logarithmic wind law that is valid in the neutral stationary surface layer. Using this result another form for K_m in the neutral case can be derived:

$$K_m = u_*^2/(\partial u/\partial z) = k u_* z \tag{11}$$

The other stability conditions, stable and unstable, are discussed separately in the following.

It can be shown that turbulence can, to a good accuracy, be described with the following three variables: friction velocity u_*, scale temperature $T_* = -(\overline{\theta' w'})_0/u_*$ and a combination g/θ, which is related to the buoyancy force. These variables can be combined into a length scale that is a measure of turbulence, called the Obukhov length

$$L = \frac{u_*^2 T_0}{g\beta k T_*}, \tag{12}$$

where T_0 is the average temperature of the surface layer. The parameter $\beta = 1 + 0.61 T_0 c_p E_0/H_0$ describes the influence of humidity to buoyancy, E_0 is the latent heat flux, and H_0 the sensible heat flux on the surface. In a stable situation $L > 0$ and in unstable situations $L < 0$.

With the help of this measure, turbulence can be simply described with two variables, z and L. Normally they are combined to a dimensionless height $\zeta = z/L$, which also is a measure of stability ($\zeta < 0$ in unstable, $\zeta > 0$ in stable and $\zeta = 0$ in neutral boundary layer).

Now, using the dimensionless wind gradient of Eq. (9), we can formulate the following equations for a non-neutral PBL

$$\frac{z}{u_*}\frac{\partial u}{\partial z} = \frac{1}{k}\phi_m(\zeta), \tag{13}$$

$$\frac{z}{T_*}\frac{\partial c}{\partial z} = \frac{1}{k}\phi_c(\zeta), \tag{14}$$

where the universal functions for momentum $\phi_m(\zeta)$ and scalars $\phi_c(\zeta)$ depend on stability, and need to be derived from observations. The boundary condition in a neutral situation when $\zeta = 0$ requires that $\phi_m(0) = \phi_c(0) = 1$. For all scalars the universal function $\phi(\zeta)$ will be the same, but the form of function $\phi_c(\zeta)$ for scalars may differ from function $\phi_m(\zeta)$ for momentum. Often-used terrestrial forms for these empirical functions are the so-called Dyer-Businger forms

$$\phi_m(\zeta) = \phi_c(\zeta) = 1 + 5\zeta \tag{15}$$

$$\phi_m(\zeta)^2 = \phi_c(\zeta) = (1 - 16\zeta)^{-1/2} \tag{16}$$

for stable ($\zeta > 0$) and unstable ($\zeta < 0$) conditions, respectively. Different forms for these functions are tested in the MPF case in **Paper II**.

From the definition of the neutral eddy viscosity coefficients (Eq. (11)) it can be seen that for stable and unstable situations the coefficients are of the form

$$K_m = \frac{k u_* z}{\phi_m(\zeta)}. \tag{17}$$

Thus, in unstable situation the coefficients are larger than in a stable case (mixing is more efficient in unstable than in neutral or stable case). Equation (17) reduces back to

Eq. (11) in the neutral case, where $\phi_m(\zeta) = \phi_c(\zeta) = 1$. Profiles for all variables, wind and scalars, can be calculated from the Monin-Obukhov vertical gradients, Eq. (13) and Eq. (14), via integration between heights z_0 and z.

3.2 The one-dimensional PBL model for Mars

The University of Helsinki 1-D PBL model is a z-coordinate column model developed for Mars by Savijärvi (1991a,b). It is based on the 2-D terrestrial σ-coordinate mesoscale model (Alpert et al., 1982; Alestalo and Savijärvi, 1985), which was also later used in Mars studies (Savijärvi and Siili, 1993; Siili, 1996; Siili et al., 1997). The 1-D model equations are

$$\begin{aligned}
\frac{\partial u}{\partial t} &= f(v - v_g) + \frac{\partial}{\partial z}(K_m \frac{\partial u}{\partial z}) \\
\frac{\partial v}{\partial t} &= -f(u - u_g) + \frac{\partial}{\partial z}(K_m \frac{\partial v}{\partial z}) \\
\frac{\partial \theta}{\partial t} &= \frac{\partial}{\partial z}(K_h \frac{\partial \theta}{\partial z}) - (p_0/p)^{R/c_p} \frac{1}{c_p \rho} \frac{\partial}{\partial z} R_{net} + (p_0/p)^{R/c_p} \frac{L}{c_p}(C - E) \\
\frac{\partial q}{\partial t} &= \frac{\partial}{\partial z}(K_h \frac{\partial q}{\partial z}) - C + E \\
\frac{\partial q_{\mathrm{ice}}}{\partial t} &= \frac{\partial}{\partial z}(K_h \frac{\partial q_{\mathrm{ice}}}{\partial z}) + C - E.
\end{aligned}$$

The pressure on all the atmospheric z-levels is calculated via the hydrostatic equation from the predicted temperature profile. The model predicts the following quantities: potential temperature θ, horizontal wind components u and v, specific humidity q, and ice mixing ratio q_{ice}. The potential temperature is defined as $\theta = T \cdot (p_0/p)^{R/c_p}$. T is the temperature, p the pressure, and p_0 the reference pressure of 7 hPa. R is the gas constant, c_p the heat capacity in constant pressure, and R_{net} is the net radiative flux (the sum of the net solar and net longwave fluxes). K_m and K_h are the turbulent mixing coefficients for momentum and heat, respectively, C accounts for condensation of water vapour into ice, and E the sublimation of water ice to vapour. ρ is the atmospheric density, and f the Coriolis parameter. u_g and v_g are the horizontal components of the geostrophic wind, and they can be used in the model to describe the flow of larger scales (from observations or climate models). The diffusion equation

$$\frac{\partial T}{\partial t} = \frac{1}{\rho c} \frac{\partial}{\partial z}(\lambda \frac{\partial T}{\partial z}) \tag{18}$$

calculates the temperature in the soil and at the surface with the predicted thermal balance (net heat flux) on the surface as a boundary condition. ρc is the volumetric heat capacity (the product of density ρ and heat capacity c) and λ the thermal conductivity of the soil. Soil moisture is not predicted but is kept constant, fixed to a value that

keeps the atmospheric precipitable water amount at the observed values. Cloud/fog water ice is formed in the model when the saturation ratio exceeds unity (relative humidity exceeds 100%). The radiative effects of the fog were not accounted for in the radiative transfer scheme, since the forming very thin fog is radiatively negligible. The assumption of critical saturation ratio of unity was tested in **Paper III** in the MPF case with the help of a nucleation model.

The number and altitude of model levels can be modified according to desired resolution. In the model runs described in **Papers I–II** there were 23 levels up to 25 km altitude with high-resolution spacing in the lowest layers of the atmosphere, and the lowest atmospheric levels were fixed to the heights of the lowest and highest temperature sensors of the MPF (0.52 and 1.27 m, respectively) to facilitate direct comparison with observations.

The turbulence scheme is based on the Monin-Obukhov similarity theory (Equations (3)-(17)) for the lowest layer and on the mixing length theory with Blackadar formulation (with an asymptotic mixing length of 300 m) above the lowest layer. The radiative transfer code in the model has been compared with line-by-line (LBL) multiple scattering calculations in average Martian conditions: thereby the gaseous longwave emissivity scheme for CO_2 and H_2O was improved, and dust was introduced via the grey approximation, as described in **Paper II**. The shortwave scheme was also improved and modified by introducing a two-stream method for Martian dust as described in detail in Savijärvi et al. (2005).

3.3 The Mars Pathfinder case and sensitivity tests with the model

Reanalyzed wind data of MPF became available in 2004 (J. Murphy, New Mexico State University, personal communication) and called for new modeling of the MPF-observed boundary layer, although the 1-D model of the University of Helsinki had produced good results on the task already (Savijärvi, 1999). Also the model had been slightly improved from the Savijärvi (1999) version, mainly by the LBL-tuned and validated radiation scheme.

3.3.1 The reference case

A reference run for the MPF case is introduced in **Paper I**, including the main modifications made to the model. The results showed a very active convective PBL during the day, dominated by radiative effects of CO_2 and dust, and a stable boundary layer with fog formation in the early morning hours. The model results compared well with the MPF data following closely the observed overall cycle of temperatures, but the

temperature gradient between the lowest atmospheric layers (the temperature sensor heights) was slightly too small (see Figure 2 in **Paper II**). The local effects of landing gear and solar panels are not taken into account in the model, and it is uncertain how they have affected the temperature observations. The model captured quite well the observed wind speeds (see Figure 2 in **Paper II**), and the model predicted a super-geostrophic nocturnal low-level jet in the morning due to inertial oscillation during the night.

3.3.2 Sensitivity tests: turbulence

The reference case introduced in **Paper I** was used in the following **Paper II** for comparison of turbulence parameterizations, testing the effect of water vapour and dust on the radiative transfer, and studying the sensitivity of the surface temperature cycle on the properties of the soil. The model was used also to produce a weather prediction for the Beagle 2 lander that unfortunately was lost during landing and did not transmit data for comparison with the model.

The turbulence scheme of the model was modified to use asymptotically correct stability functions for very unstable situations (Delage and Girard, 1992), which also resolve correctly the matching between the surface layer and the Ekman-layer (the layer above the surface layer where fluxes can not be considered constant anymore). The model results using the formulae of Delage and Girard (1992) and the popular Dyer-Businger forms (DB, Dyer, 1974) were compared to the MPF wind data. Even though the Martian surface layer is very unstable during daytime, the DB forms, at least in this case, were describing the behaviour of turbulence well enough. Perhaps the backgroud wind used also helped in keeping the wind profile well-mixed in the model during the day. However, also Delage and Girard (1992) pointed out that their form for the universal function for momentum ϕ_m did not produce significant changes in the kinematic stress calculated with their model. The function ϕ_h has an effect mainly in the fluxes of latent and sensible heat, which we did not study in detail with our model, and which are small in the Martian surface layer. These points may explain at least partly why our results were not particularly sensitive to the forms of functions ϕ_m and ϕ_h.

An iterative surface layer (using the DB-functions) was also introduced, where the surface heat fluxes and the Obukhov length were iterated until convergence (heat fluxes within 0.001 W/m^2). The iteration did not change the results, probably due to the short timestep of 10 s used in the model, which already ensures frequent updating of the variables.

3.3.3 Effects of water vapour and dust on radiative transfer

The effects of variable water vapour and dust on the downwelling longwave radiation (DLR) and on surface and near-surface temperatures were also tested in **Paper II**. The main result was that water vapour has an effect of 10% on the DLR throughout the sol in the MPF case with 25 precipitable microns of water. The effect of dust ($\tau = 0.3$) was about 25%, and the two together account for about one third of the DLR. The DLR has a big effect on the surface and near-surface temperatures (see Figure 4 in this section, and Table I and Figures 4 and 5 in **Paper II**). Especially during the night, when the DLR dominates the surface radiative balance, water vapour has a significance in increasing surface temperatures, as does dust (2–3 K). During daytime the DLR-effect is similar, but now dust also acts as an absorber and scatterer of solar radiation, and thus shadows the surface. This leads to an overall effect of higher daytime surface temperatures with less dust in the atmosphere, and lower surface temperatures with higher atmospheric dust amounts. The atmospheric temperatures at 1.3 m, however, behave differently. Without dust the daytime temperatures are clearly lower than in the dusty case, since dust is not absorbing the longwave radiation emitted by the hot surface and the spectral window of the dust-free CO_2 atmosphere is wide. With the strongly absorbing dust in the atmosphere the air temperatures are higher. Thus the diurnal temperature cycle is damped on the surface by a dusty atmosphere, as seen also in the VL observations (Ryan and Henry, 1979). In the atmosphere, however, the whole cycle gets warmer than without dust. This effect of dust is significant also in the formation and development of dust devils in the Martian atmosphere, since the absorption of solar and longwave radiation enhances the circulation in them (Fuerstenau, 2006).

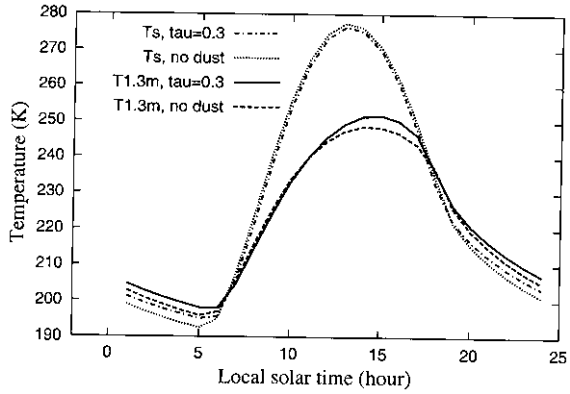

Figure 4: The 1-D model results in Pathfinder conditions, season L_s=140°, for the effect of dust on surface (higher curves) and lowest model level (lower curves, 1.3 m altitude) temperatures with no dust and well-mixed dust with visible optical depth of $\tau = 0.3$.

Also the effect of solar zenith angle in dusty conditions was investigated by modeling the onset conditions of the first autumn dust storm observed by Viking Lander 1, when the slant solar radiation travels a longer way through the dusty atmosphere and is consequently attenuated. We tested dust optical depths of $\tau = 0.5$ (onset of the storm) and $\tau = 3.0$ (during the storm). The model reproduced a 10 K decrease in the 1.3 m daytime maximum temperatures and a 5 K increase in the nighttime minimum temperatures, as was observed by the lander (Ryan and Henry, 1979).

3.3.4 Properties of the surface: effect on the diurnal surface temperature cycle

The UH 1-D model was used in **Paper II** to investigate the effect of surface properties and surface heat fluxes on the ground temperatures predicted by the model. The surface heat fluxes were neglected in the model that was used in retrieving thermal inertia values from the observations of TES/MGS (Mellon et al., 2000). The heat fluxes are included in the UH 1-D model used in **Papers I–II**. Our goal was to estimate the possible error made in the thermal inertia retrieval. However, most probably because of the weakness of heat fluxes in the thin atmosphere, they do not impose a large effect on the surface temperatures: the two models agreed fairly well with a large range of thermal inertia values (to 1-2 K). An example of the results of the 1-D model is shown in Figure 5, which is a reproduction of Figure 1 in the article of Mellon et al. (2000).

The thermal inertia $I = \sqrt{\rho c \lambda}$ is the root of the product of the volumetric heat capacity of the soil ρc (where ρ is the density and c the heat capacity) and the soil thermal conductivity λ. Thermal inertia can be retrieved from orbital observations of diurnal cycle of surface temperature, but its components, heat capacity and thermal conductivity, are not as straightforward to deduce. We tested the possibility of using the 1-D model and MPF observations to derive the most likely behaviour of the two properties of the soil. In the above comparison with Mellon et al. (2000) the heat capacity ρc was kept constant and the thermal conductivity λ varied to produce the required values of I. We tested the sensitivity of surface temperatures on the variation of both properties while keeping I constant: constant I suggests constant amplitude and phase of the diurnal surface temperature variation. However, with changing the values of ρc and λ have an effect on the shape of the curve. Indeed, it appeared that surface temperatures respond more strongly to variations in thermal conductivity λ than in variations of heat capacity ρc. With ρc halved and λ doubled from the reference values, surface temperatures in the afternoon stay too low, fall quickly, and stay nearly constant throughout the night. If ρc is doubled and λ halved, the fit is better, but the afternoon peak temperatures are still too low, and the surface stays too warm during the night. Thus it seems that the realistic range for the heat capacity ρc in the MPF site is near the reference value of $0.8 - 0.9 \cdot 10^6$ J m^{-2} K^{-1}, and the value of thermal conductivity λ can be adjusted to achieve the desired value of thermal inertia

I. It would be interesting to study this matter further with other lander observations to compare with locations with different soil properties.

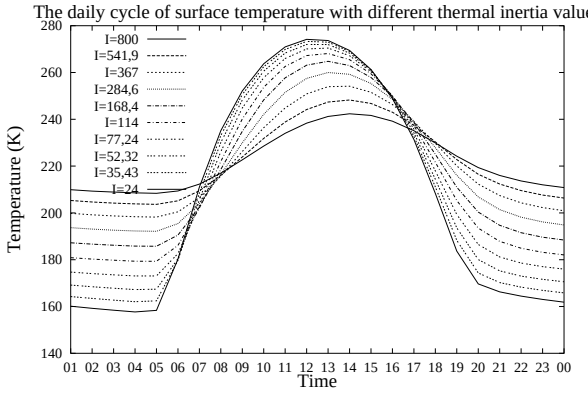

Figure 5: The effect of thermal inertia (W m^{-2} s$^{-1/2}$ K^{-1}) to the daily cycle of surface temperatures according to the 1-D model. ρc was kept constant and only λ was varied.

3.3.5 Beagle 2 landing site climate

Paper II presents model runs of average monthly climatic conditions for the unsuccessful Beagle 2 lander landing site (the planned landing ellipse was centered at 11.6°N, 269.5°W). The model was initiated with data from the Mars Climate Database (MCD, Lewis et al., 1999), mainly for geostrophic wind, surface pressure, and temperature. Dust opacity and precipitable water vapour amounts were fixed according to the MGS/TES observed values.

The Beagle 2 model predictions showed mild, temperate climate with little variation in the tropical temperature through the year, winds were tradewinds typical to the tropics (related to the Hadley cells), and even above-zero temperatures (2.3°C) were reached in the model runs. Saturated conditions were reached for short periods during the night, but no significant fog formation occurred. Also Bingham et al. (2004) published an article on the Beagle 2 landing site weather according to the MCD, and their conclusions mostly agree with our results. They predicted a surface pressure rise during the mission, which is seen in our input data (taken from the MCD as well), but the predicted surface temperatures for the approximate time of landing from the 1-D model are slightly higher (maxima 275.5 K vs. 268 K) than those of the MCD. Bingham et al. (2004) used the MGS-scenario to describe the dust optical depth, and we also used the MGS results, but it is possible that the values differ, influencing the temperature prediction. Our model also predicted stronger winds at the surface at 13:00 local time (8 m/s at 1.4 m vs. 5 m/s at 4 m by Bingham et al. (2004)). Their 5 m wind reached 8 m/s in the dust

storm case of maximum optical depth of $\tau = 5$. Wind maxima for the MGS-scenario were reached at 16:00 local time in the beginning and the end of the mission, whereas our maxima were reached closer to noon, at around 13:00 local time. Unfortunately no data arrived from the lander for comparison with the results.

4 Nucleation in the Martian atmosphere

The Martian clouds have been concluded to form from H_2O (more frequently) and from CO_2 (rarely), since they are the two volatiles condensing on the polar ice caps, and since the observed temperature regimes imply the same to happen also in the atmosphere. The cycles of water, CO_2 and dust have been briefly reviewed in Section 2.3 and clouds and fogs of Mars in Section 2.6. Section 2.2 mentions observations of clouds and fogs on Mars. In the following the focus is on the cloud formation process itself. Nucleation theories, both homogeneous and heterogeneous, and both one- and two-component, are here reviewed briefly. A more accurate description can be found in **Papers III-V**.

The first step in particle formation is nucleation, which involves a phase transition. In an atmosphere the transition occurs from vapour phase to solid or liquid clusters of molecules, but in a liquid nucleation can also happen from liquid to gas (like bubbles in a lemonade bottle) or liquid to ice (when opening a supercooled lemonade bottle or when a supercooled water droplet encounters another aerosol particle, or any surface, like the wing of an aeroplane). On Mars there is no liquid phase for substances in the atmosphere, so the transition happens from vapour to solid (ice). In general, the clusters can form either directly from the vapour phase, or they can form on a pre-existing surface. The processes are called homogeneous and heterogeneous nucleation, respectively. Homogeneous nucleation requires more energy, since there is more new phase-separating surface to be created. Heterogeneous nucleation is easier because the pre-existing particle (condensation nucleus/nuclei, CN) provides a part of the surface. However, in some situations pre-existing surfaces are not available, in which case homogeneous nucleation may occur. On Mars the ubiquitous dust acts as the CN, and most probably clouds on Mars form via heterogeneous nucleation since dust is readily available in nearly all conditions. The formation of clouds may also happen so that first the H_2O crystals form on the dust, and later on CO_2 can nucleate on the water ice crystals: the efficiency of water ice as a seed seems to be better than that of Mars analog minerals (Gooding, 1986). Thus cloud formation on Mars is a link between the major climatic cycles of water, CO_2 and dust, exhibiting highly nonlinear behaviour (Michelangeli et al., 1993; Rodin et al., 1999) that affects radiative transfer, and through it, the atmospheric circulations.

4.1 Nucleation theory

4.1.1 A summary of nucleation thermodynamics

Here and in **Papers III-V** the classical nucleation theory is briefly reviewed. A more detailed description of nucleation theory can be found in Volmer (1939), Reiss (1950),

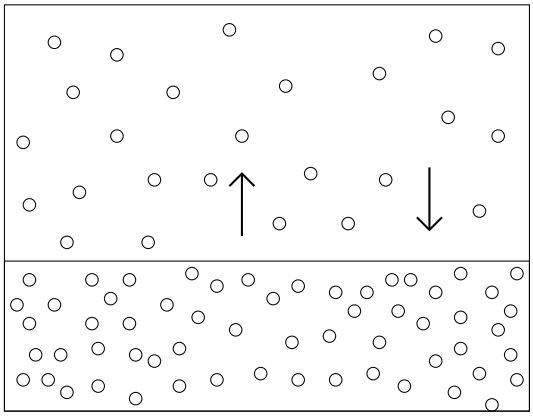

Figure 6: A schematic plot of the equilibrium state for a one-component system. The vapour phase is in saturation ($S = 1$) and the fluxes to and from the source exactly balance.

Fletcher (1958), Stauffer (1976), Trinkaus (1983), Keesee (1989), Pruppacher and Klett (1997), and Vehkamäki (2006).

There are always clusters in a vapour, but only some of them reach sizes that are favorable to growth. These clusters are called critical clusters, and properties related to them are from now on marked with asterisk as superscript (*). The concepts of saturation ratio, gas phase activity, equilibrium and supersaturation are important in the following, and are briefly explained here. In a closed container of liquid (or solid) and vapour of the same substance an equilibrium (saturation) is reached when the vapour fluxes to and from the liquid (solid) source exactly balance (see Figure 6). If the vapour is subsaturated (less vapour than in the equilibrium state), the flux from the source grows so that equilibrium is reached. If the vapour is supersaturated, the balancing flux is from the vapour to the source. However, in an atmosphere there may not necessarily be a liquid or solid surface available to help maintain equilibrium, and thus super(or sub)saturated state can form and prevail. Saturation ratio S_i, gives the ratio of the partial pressure of the vapour to the equilibrium vapour pressure in given conditions, so it tells how far from equilibrium ($S_i = 1$) the system is. The saturation ratio is defined as $S_i = p_i/p_{\mathrm{sat}}$. p_i is the partial pressure of the nucleating vapour and p_{sat} is the saturation vapour pressure of the substance at temperature T. In a multicomponent system the source can be defined either as the liquid or solid mixture or as the pure substance: the gas phase activity $A_{g,i} = p_i/p_{\mathrm{sat,pure}}$ describes the saturation state of a system over the pure substance, whereas saturation ratio $S_i = p_i/p_{\mathrm{sat,mix}}$ uses the mixture as a reference state (see Figures 7a and 7b).

The process that is required to balance supersaturation towards an equilibrium state is nucleation, and critical clusters can form in a supersaturated state, provided some conditions are met; these conditions will be described in the following.

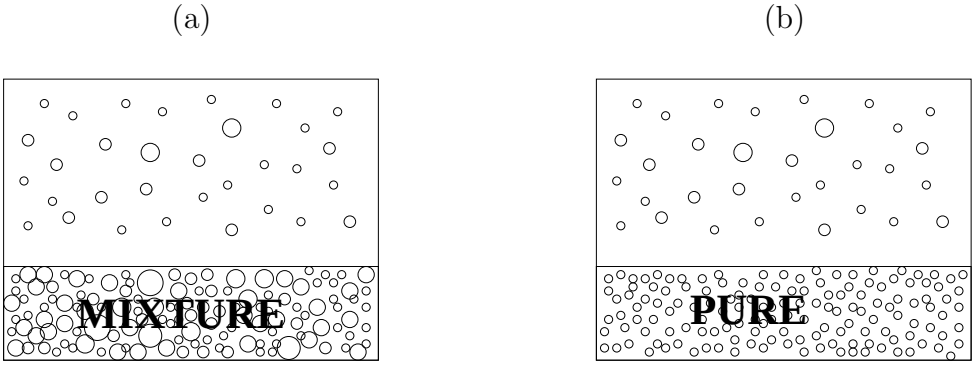

Figure 7: Schematic plots of the definitions of a) saturation ratio S_i (the liquid/solid pool is the mixture), and b) gas phase activity $A_{g,i}$ (the liquid/solid pool is the pure substance i) in a multicomponent system.

The critical size is the size after which the growth of clusters is thermodynamically favoured. The formation of critical clusters depends on reaching the top of the barrier in Gibbs free energy of formation (Figure 8), linked to the saturation state of the vapour. Figure 8 shows the Gibbs free energy of formation as a function of molecules in the cluster: the critical size is found at the peak of the curve (where the derivative is equal to zero). The barrier (critical formation energy) is lower and the critical cluster smaller for larger saturation ratios. In the homogeneous case the critical formation energy reads

$$\Delta G^*_{\mathrm{hom}} = \frac{4}{3}\pi r^{*2}\sigma_{g,l} \tag{19}$$

where r^* is the radius of the critical cluster, given by equation

$$r^* = \frac{2\sigma_{g,l}v_i}{kT\ln S_i}. \tag{20}$$

In these equations $\sigma_{g,l}$ is the surface tension (surface energy) between gas (g) and liquid or solid (l) phases. A notation l=liquid is used here for the cluster even though the condensed phase can be either liquid or solid: however, in terminology it is better to separate the cluster from the solid pre-existing particle, the condensation nucleus. v_i is the molecular volume in the condenced phase of species i, k is the Boltzmann constant, T is the temperature and S_i the saturation ratio. The denominator of Eq. (20) is the chemical potential difference between gas and liquid at the gas pressure for ideal gas

$$\Delta\mu_i = -kT\ln S_i. \tag{21}$$

The number of molecules in the critical cluster can be calculated from the volume of the cluster and density of liquid/solid

$$N^* = \frac{4}{3}\pi r^{*3}\rho_l, \tag{22}$$

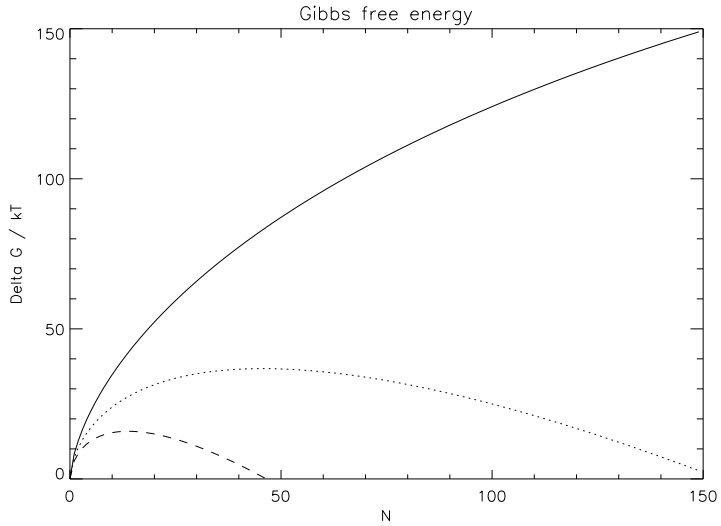

Figure 8: The Gibbs free energy of formation as a function of number of molecules for temperature T=280 K and saturation ratios of S= 2 (solid line), 5 (dotted line), and 10 (dashed line).

assuming that the density of bulk liquid/solid, ρ_l, can be used to describe the density of the cluster.

The above formula of the radius holds for both homogeneous and heterogeneous nucleation, but the formation free energy of the heterogeneous cluster,

$$\Delta G^*_{\rm het} = f_g \Delta G^*_{\rm hom}, \tag{23}$$

is reduced from the homogeneous case (19) by a geometric factor f_g. The number of molecules in the heterogeneous cluster is related to the homogeneous case through another geometric factor, f_n, as $N^*_{\rm het} = f_n N^*_{\rm hom}$. These geometric factors are simply derived from the cluster-substrate geometry, see Fig. 9 and **Papers III-V**. In Figure 9 $R_{\rm CN}$ is the radius of the pre-existing particle and r^* the radius of the critical cluster. The angle θ is the contact angle between the liquid/solid and the pre-existing particle, and its cosine, the contact parameter $m = \cos\theta$ is defined by Young's equation as

$$m = \cos\theta = \frac{\sigma_{g,\rm sol} - \sigma_{l,\rm sol}}{\sigma_{g,l}} \tag{24}$$

where $\sigma_{g,\rm sol}$ is the surface tension between the gas and pre-existing solid phases, and $\sigma_{l,\rm sol}$ is the surface tension between the liquid/solid and pre-existing solid phases.

In two-component nucleation the numbers of molecules of the two species in the cluster core and on the surface may differ, since some substances are more surface active

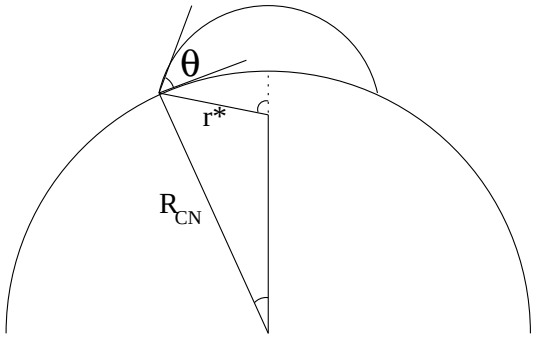

Figure 9: The geometry of heterogeneous nucleation: a critical cluster of radius r* on the surface of a pre-existing particle of radius R_{CN}. θ is the contact angle.

(prefer to accumulate to the surface) than others. Thus the numbers of surface and core molecules need to be calculated separately. The number of core molecules (the molecules in the cluster not belonging to any of the cluster surfaces) in the cluster is given by

$$N^* = \frac{4}{3}\pi r^{*3} x_{i,l} \rho_l(x_{i,l}, T), \tag{25}$$

where the density ρ_l is the density of the bulk mixture, and $x_{i,l}$ is the mole fraction of the species i in the critical cluster core, which can be iteratively solved from the equality

$$\frac{\Delta\mu_1(x_{i,l})}{v_1(x_{i,l})} = \frac{\Delta\mu_2(x_{i,l})}{v_2(x_{i,l})}. \tag{26}$$

The calculation of the numbers of molecules in the cluster surfaces on gas-liquid (g, l) and liquid-solid (l, sol) interfaces is described in **Paper V**. The total number of molecules in the cluster is thus the sum of core molecules, given by the predicted mole fraction in the cluster, and surface molecules, depending on the areas of the surface interfaces.

4.1.2 Nucleation rate and nucleation probability

Nucleation is often measured as the amount of nucleated clusters per unit time in a volume, on a surface area, or per pre-existing particle, defined as the nucleation rate J. A general form for the nucleation rate is given by

$$J = R_{\mathrm{av}} Z F^e \exp\left(\frac{-\Delta G^*}{kT}\right), \tag{27}$$

which consists of two parts: the kinetic prefactor ($R_{\mathrm{av}} Z F^e$) and the thermodynamic exponential part. In the kinetic prefactor R_{av} is the average growth rate of the cluster,

Z is the Zeldovich factor, and F^e is the equilibrium concentration of monomers (a monomer is a single, unbound molecule as opposed to dimers, which are clusters of two molecules bound together, trimers, etc.). The different formulations for components of Eq. (27) are described in detail in **Papers III-V**, and are only qualitatively reviewed here.

First, however, a word on units. The units of nucleation rate J for homogeneous nucleation are normally $\mathrm{m}^{-3}\mathrm{s}^{-1}$, i.e. formed clusters per cubic meter per second. These units are not, however, very practical for describing heterogeneous nucleation, since the number of nucleated clusters per cubic meter depends then on the concentration of CN in the volume of air. Thus more often units of $\mathrm{m}^{-2}\mathrm{s}^{-1}$ or s^{-1} are used, meaning nucleated clusters per pre-existing particle surface area per second, or per (pre-existing) particle per second, respectively. Values of nucleation rate J in these units are not dependent on the amount of CN. An even more useful measure is the nucleation probability (see, e.g. (Lazaridis et al., 1992)). It is defined as

$$P = 1 - (JA_{\mathrm{CN}}t) \tag{28}$$

where J is given in $\mathrm{m}^{-2}\mathrm{s}^{-1}$, A_{CN} is the substrate surface area and t is the time interval during which nucleation is assumed to happen (normally of the order of 10^{-3} s). The nucleation probability describes the cluster-forming potential of the vapour and is not dependent on the number of CN: but it does give the fraction of the CN that are activated in nucleation in the prevailing conditions, and is thus very useful for cloud formation studies. Thus, the concept of nucleation probability P is more general than nucleation rate J. The concepts of onset and critical saturation ratio are used often presenting the results of the model runs. Onset of nucleation is defined to happen when a certain threshold nucleation probability P is reached. This threshold is in my studies defined as $P = 1$ (**Papers III-IV**) or $P > 0.5$ (**Paper V**). The critical saturation ratio is the value of saturation ratio S_i at which the onset happens.

4.1.3 A summary of nucleation kinetics

The kinetic prefactor consists of three components, R_{av}, Z, and F^e, as described above. Each of the components is described here briefly, and the different kinetic models are qualitatively reviewed.

At the critical size a cluster can grow if it acquires a monomer. It can also lose a monomer, become subcritical, and decay. The critical cluster concentration in the vapour needed to derive Eq. (27) is calculated for equilibrium conditions, but nucleation takes place in supersaturated vapour. The Zeldovich factor Z accounts for the aforementioned two effects: the possible break-up of critical clusters, and the difference between the equilibrium vapour and the nucleating (supersaturated) vapour. The Zeldovich factor involves calculating second derivatives of the free energy with respect

to the number of molecules in the cluster. In the one-component case this is very straightforward, but in the two-component case it requires numerical calculation of the derivatives with respect to the total molecular numbers in the critical cluster (the sum of surface and core molecules). The heavy numerics of solving the second derivatives in the two-component case can be avoided by approximating the Zeldovich factor, for example, with the help of an extension of the one-component Zeldovich factor by describing the monomer colliding with the cluster as an "average" of the monomers of the two species. The Zeldovich factor for one-component heterogeneous nucleation is described in detail in **Paper IV**. The different exact and approximate approaches for calculating the Zeldovich factor in two-component nucleation are listed and applied in **Paper V**.

The number of monomers F^e in the homogeneous case is the equilibrium monomer concentration in the vapour, whereas in the heterogeneous case it is calculated as the number of monomers on the unit substrate surface. The latter can again be calculated in two ways: the surface can be assumed to be totally covered by monomers (monolayer assumption), or the concentration can be calculated from a steady-state between incoming and outgoing fluxes of monomers. The effect of the approach chosen is studied in more detail in **Paper III**. For two-component nucleation studied in **Paper V** the monomer number concentration is approximated as the sum of the monomer numbers of the two components, and the steady-state approach is used.

The average growth rate R_{av} can be related to direct collisions of monomers with the critical cluster (homogeneous nucleation and the direct vapour deposition approach of heterogeneous nucleation, DVD), or to diffusion of monomers to the cluster on the pre-existing particle surface (surface diffusion approach in heterogeneous nucleation, SD). For description of both processes see, for example, Pruppacher and Klett (1997), and the schematic pictures of Figures 10a and 10b. Naturally in reality both processes are working simultaneously (see Figure 11), but the surface diffusion process is significantly faster than the direct vapour deposition, and thus the latter can be neglected in most cases. In two-component nucleation the Gibbs free energy of formation is a saddle surface in molecular number space, and the cluster has to overcome a barrier at the saddle point. However, the direction most favorable for growth does not necessarily coincide with the saddle point (this being the simplest approach), but may curve on the slopes due to kinetics. This needs to be taken into account by calculating the collisions/diffusion in that direction. The direction angle of growth in the two-dimensional size space of the two-component cluster can be calculated exactly or with varying levels of approximations, for example with the help of mole ratios in the critical cluster. The approximations are described and compared to the exact solution in **Paper V**.

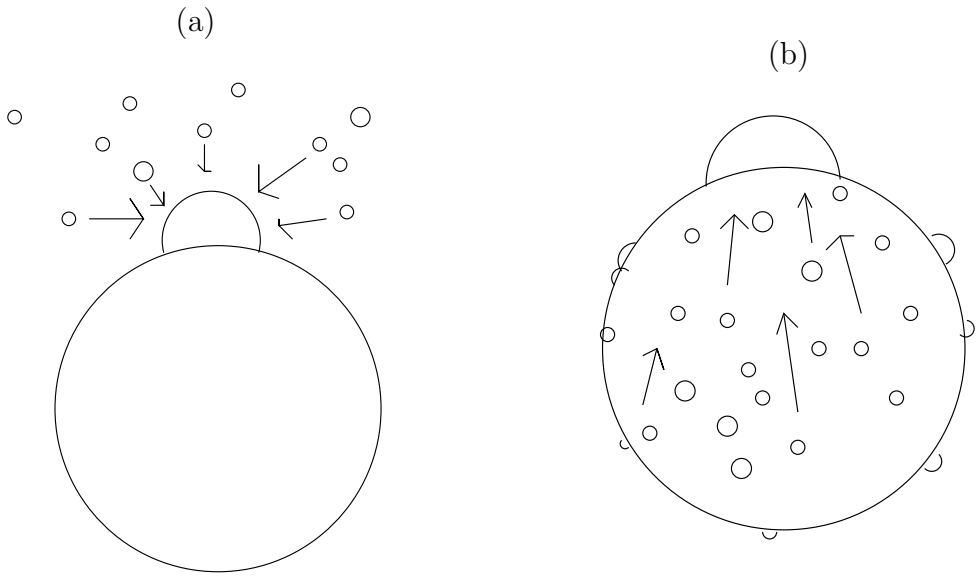

Figure 10: Schematic plots of the two models commonly used for the growth of the critical cluster: a) direct vapour deposition, and b) surface diffusion.

4.1.4 Nonisothermal effects

In the Martian atmosphere CO_2, forming 95.3% of the atmosphere, may take part in cloud formation. Thus the process takes place in near-pure vapour: in the absence of a carrier gas. This needs to be taken into account at least in homogeneous nucleation and in condensation. In the presence of a carrier gas frequent collisions with inert molecules carry away the energy related to the phase transition, and the cluster formation can be considered isothermal. In a near-pure situation the amount of monomers adhering to the cluster far exceeds that of the inert monomers only colliding with it, and the released latent heat warms the cluster, slowing down the nucleation process (Feder et al., 1966). However, in heterogeneous nucleation the CN acts as a heat bath thermalizing the cluster efficiently, and nonisothermal correction is not required.

In **Papers III-IV** the nonisothermal correction is taken into account also in heterogeneous nucleation, as was done in the work of Wood (1999), on which the studies of **Papers III-IV** are based. However, in **Paper V** the correction is omitted as unnecessary in heterogeneous nucleation, but it is also shown that the effect of the correction is negligible. The nonisothermal theory is mentioned here briefly since it is used in the papers included in this thesis. It should also be noted that in the case of heterogeneous nucleation in near-pure vapour on very small CN (smaller than the cluster itself) the correction may need to be taken into account, as well as in ion-induced nucleation, since in these situations the CN is too small to thermalize the cluster effectively.

The nonisothermal correction for nucleation in near-pure vapour is described by Feder

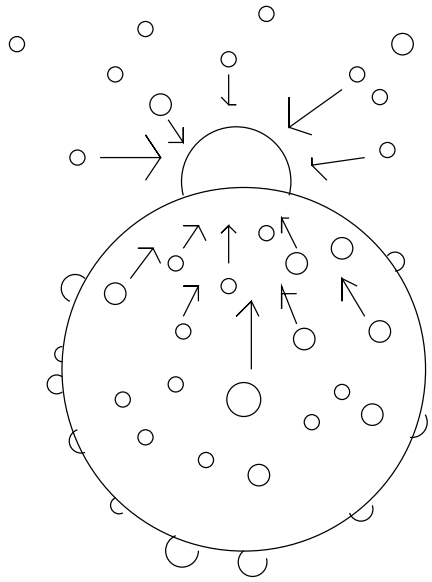

Figure 11: A schematic picture of the combination of the two growth models (direct vapour deposition and surface diffusion).

et al. (1966). Since the release of latent heat in the nucleation process is not transported away in lack of a carrier gas, the cluster heats up, and the nucleation rate is slowed down with a factor $f_{\delta T}$

$$f_{\delta T} = \frac{b^2}{b^2 + q^2} \tag{29}$$

where b is the energy lost when gas molecules collide with the cluster but do not adhere to it, and q describes the energy acquired by the cluster with adhered monomers of the nucleating vapour. The equations for b and q are described more in detail in **Paper III** and **Paper V**.

4.2 Sensitivity of the heterogeneous nucleation rate

Calculation of the heterogeneous nucleation rate depends not only on the atmospheric state (temperature, pressure, vapour amount, and so on) but also on the theoretical approach used, and the properties of the CN. However, it should be noted that the onset of nucleation is not very sensitive to the factors described here.

The kinetic prefactor in Eq. (27) for the nucleation rate consists of three parts: the Zeldovich factor, the average growth rate (the growth model) and the equilibrium concentration of monomers. As mentioned in Section 4.1.3, the growth model used for the cluster can be chosen from two generally used formulations called the direct vapour deposition (DVD) and surface diffusion (SD). Theoretically (Pruppacher

and Klett, 1997) the difference in the resulting nucleation rates is of the order of $\exp[(\Delta F_{\rm des} - \Delta F_{\rm sd})/kT]$, the surface diffusion rate being faster. The difference was 10^5–10^8 in the temperature range of our Mars model runs (see **Paper III**). In addition to the growth model, also the Zeldovich factor includes the growth direction angle (see Section 4.1.3). For two-component nucleation the kinetics of nucleation using the exact theory requires heavy numerics, since both the growth direction angle of the cluster on the Gibbs free energy surface and the exact Zeldovich factor require the second derivatives of the Gibbs free energy taken with respect to the total number of molecules in the cluster. The exact solution and different approximations are compared in **Paper V**. However, it should be mentioned here that for heterogeneous nucleation probability the choice of Zeldovich factor, growth model and angle is not so crucial, as discussed in **Paper V**. Nucleation probability is dominantly affected by the exponential of the free energy, whereas the growth model and Zeldovich factor only appear in the kinetic prefactor, thus having only a minor effect on the prediction of onset conditions.

The description of the amount of clusters and growth of the clusters requires information on the amount of available monomers. The different choices (the monolayer assumption and the steady-state approach) for describing this are reviewed in Section 4.1.3, and they are discussed in **Paper III**. Naturally the monolayer approach combined with surface diffusion gives the maximum nucleation rates. Note here that despite its name the surface diffusion does not assume a monomer gradient that drives the flow, but it only requires a source of monomers that will anyway jump to try and join the cluster. Thus the monolayer is the maximum monomer source for the surface diffusion growth rate. The monolayer assumption represents the maximum of monomer concentration, but is quite unrealistic, since there is really no need for nucleation if the whole CN is already "wet" with molecules. The slowest nucleation rates are achieved with steady-state monomer concentration and direct vapour deposition. The steady-state approach is more realistic, but most probably the flux of monomers to the cluster along the surface is much faster than the replenishing flux of monomers from the vapour to the surface, and thus this approach should be still re-evaluated.

The CN size affects the nucleation rate, since nucleation is facilitated, to some extent, by larger particle sizes. The models presented in **Papers III-V** utilize a monodisperse size distribution, which means they use pre-existing particles of only one size. However, the change of CN sizes with altitude in the atmosphere (due to sedimentation) was taken into account in **Paper III** by introducing a CN size profile, where the CN diameter changed according to a factor calculated by a deposition model for Martian dust (Merikallio, 2003). The deposition model showed that the dust radius decreases with a factor of 2 when going up to 20 km. The smaller the particles are, the more difficult nucleation is, and thus higher up in the atmosphere the use of large particles would give unrealistic nucleation rates. Our model using this simplified altitude profile of dust size agreed well with a full aerosol model of Colaprete et al. (1999) that used a full size distribution description, and we predicted H_2O nucleation also above 40 km

where their model predicted H_2O cloud formation. However, without the correction of dust size change with height, our predictions could have given unrealistically thick layers of nucleation at high altitudes.

One note to make is that the contact angle θ (or contact parameter $m = \cos\theta$), given by Young's equation (Eq. (24)), is very poorly known for the Martian cases. Also the surface tensions required in Young's equation (Eq. (24)) are not known. We used values of m evaluated by Michelangeli et al. (1993) for water and measured by Glandorf et al. (2002) for CO_2, but there is not enough information on the minerological composition of Martian dust to derive the contact angles, and the laboratory experiments of Glandorf et al. (2002) were made with CO_2 nucleating on a water ice film, not on a mineral substrate. These evaluations are anyhow the best data available at the moment for the contact angles in Martian nucleation. Another point is that even though classical nucleation theory assumes spherical shape for both liquid and solid clusters, the real phase and the shape of a cluster containing few or few tens of molecules are not necessarily well defined and the concept of contact angle describes more the interaction of the cluster and the surface and the properties of the surface than a real angle.

4.3 Summary of results on nucleation in the Martian atmosphere

4.3.1 One-component nucleation on Mars

Our models of homogeneous nucleation showed that formation of clusters directly from the vapour phase requires very large saturation ratios, up to 10^5–10^7, implying very low temperatures that have not been observed in the Martian atmosphere. Another point is that CN for heterogeneous nucleation are readily available on Mars because of the well-mixed, ubiquitous dust. Thus the evident conclusion is that homogeneous nucleation can not be the dominant pathway of ice crystal formation on Mars in its present, dusty climate.

Heterogeneous nucleation thus is the most probable pathway for ice crystal formation on Mars, and models were developed to describe both H_2O and CO_2 nucleation. The results from the heterogeneous nucleation models agreed with previous modeling (Inada, 2002; Colaprete et al., 1999) and with laboratory experiments (Glandorf et al., 2002). The model of Inada (2002) used a different theoretical approach for describing the monomer concentration and growth of the cluster. These approaches were tested with our model, and the results agreed within two orders of magnitude in nucleation rates when differences in theory were removed. The remaining difference was related to the model of Inada (2002) using a polydisperse CN size distribution, whereas that of our model was monodisperse.

The basic runs for near-surface conditions (p_s=6 hPa, T=100-300 K) showed that water (300 ppm in vapour phase) starts nucleating at around 200 K on 1 μm radius dust particles when saturation ratio exceeds 1.18. This result was consistent with subsequent studies of modeling nucleation with the Mars Pathfinder entry profile, as in Colaprete et al. (1999), and the nucleation model predicted ice crystal formation at the same altitudes as the full cloud model of Colaprete et al. (1999).

For CO_2 the model predicted onset of nucleation at nearly the same saturation ratio as shown by the experiments of Glandorf et al. (2002), which is the only dataset so far available for nucleation in Martian conditions. We used the contact angle derived from their experiments, but our approach for nucleation theory (surface diffusion on a spherical CN). The model-predicted onset saturation ratio agreed well with the observed one, and the small discrepancy in the results was related to the differences in the theoretical approaches used and the experimental set-up.

The model for water was used also to study cloud and fog formation in different locations as a function of altitude. The surface fogs have only been observed from imaging or indirectly speculated from lander observations, so the efforts of modeling studies were mainly concentrating to reveal if fog formation at those locations during that season would be possible, and if so, what fog properties and settings for onset of nucleation the models predict. To do this, atmospheric profiles were required, and one of them was the aforementioned Mars Pathfinder entry profile. The other profiles were produced with the 1-D model of the University of Helsinki, the same model that was used in the PBL studies of **Papers I–II**. The fog formation at the Mars Pathfinder landing site was predicted as before by simpler condensation schemes (e.g. Savijärvi, 1999; Savijärvi et al., 2004), but nucleation took place in a shallower layer than previously modeled, since the required saturation ratios are not equal to, but exceed, unity. The surface fog at Memnonia region observed by Viking Orbiter 1 (Briggs et al., 1977) was modeled and the model results compared to those of Inada (2002). Our model predicted nucleation in a shallower layer than the saturated layer predicted by Inada (2002), which is again due to the significant supersaturation required for nucleation. The layer where nucleation was expected was 100 m deep in our model runs and persisted through the morning hours. The fog thickness can not be deduced from VO1 observations, so direct comparison with observations is not possible. However, the models did show that fog formation is possible at both locations, the MPF landing site and Memnonia region. The MPF entry profile was used to compare our model with the full aerosol model of Colaprete et al. (1999), and our model predicted H_2O nucleation at the altitudes where the model of Colaprete et al. (1999) implied water ice cloud formation to take place.

Our goal was also to study CO_2 cloud formation in the polar night, but the profiles of the Mars Climate Database (Lewis et al., 1999) were inapplicable, since supersaturation is not allowed to form in the general circulation model results that are included in the database.

The developed nucleation models worked well in comparison to data and other modeling, and they were later on developed further by removing any approximations still left via the derivation of the accurate Zeldovich factor in **Paper IV**. The model runs in the CO_2 case of **Paper III** were rerun, and it was shown in **Paper IV** that the results do not change much for large CN (R_{CN} =1 μm, as used in **Paper III**), but the difference can become significant for CN radii smaller than 100 nm.

The nucleation models developed are light, analytical models, that can be used to calculate required critical saturation ratios in atmospheric models. For the cloud climatology to be correctly predicted, correct onset saturation ratios are important: using a critical saturation ratio of unity overestimates the frequency of cloud formation and distorts the climatology in a climate model, since in reality the saturation ratios required are significantly higher than unity.

4.3.2 Two-component nucleation on Mars

Encouraged by the studies of multicomponent nucleation on Earth and clathrate formation on Mars mentioned in the end of Section 2.6, we started working towards possible two-component nucleation of H_2O and CO_2 on Mars. It should be pointed out here that the classical nucleation theory does not predict anything about the forming crystal structure or possible chemistry involved in the process: only the bulk thermodynamic properties used for the substances and the mixture may implicitly contain such information, if they have been properly measured. Often such measurements are not available, as is the case for Mars, and thus assumptions need to be made. Crystal growth experiments, and measurements or more detailed modelling of the properties of the substances are needed to define more accurately the full nature of the multicomponent clusters and subsequent crystals. A two-component homogeneous nucleation model using the kinetics of Stauffer (Stauffer, 1976; Trinkaus, 1983) was modified for heterogeneous nucleation and applied to a test system of laboratory measurements of water and *n*-propanol (Wagner et al., 2003), and compared to previous modeling results (Kulmala et al., 2001). After these tests it was modified for Martian conditions.

The comparison to the experimental data and previous modeling brought up the question of different approaches to the kinetics of two-component nucleation, which became another main topic of **Paper V** along with the Martian test case. The model used in Kulmala et al. (2001) included several approximations mentioned earlier in Section 4.1.3. Those approximations, namely the direction angle of cluster growth and the Zeldovich factor, were tested against the experimental data. According to the results the approximations do not affect the prediction of nucleation onset, which is mainly sensitive to the exponential of the Gibbs free energy, and not so much to the kinetic prefactor containing the growth angle and the Zeldovich factor. In the comparison both

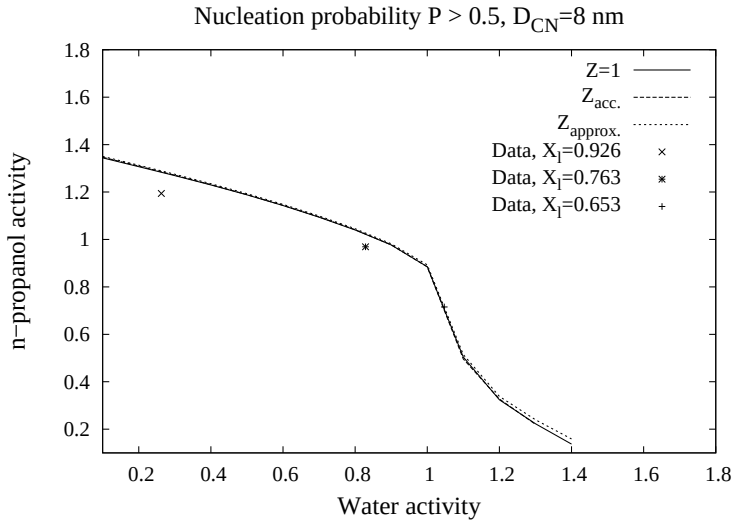

Figure 12: An activity plot showing the two-component nucleation model results for CN of 8 nm diameter for all used models and the experimental data for three different mass fractions X_l of n-propanol. The lines depicting the model results nearly overlap and are thus fairly indistinguishable.

models reproduced the observed behaviour of the system qualitatively well (Figure 12), but failed to match the data quantitatively.

Anyhow, the small difference between the predicted onset activities for the laboratory system and the experimental data is insignificant compared to the possible errors produced by the assumptions that had to be made for the Martian H_2O – CO_2 system. There is no thermodynamic data available for this system, and thus all the properties had to be estimated, for example, by interpolating the properties of the pure components. We tested two approaches. The first was the ideal mixture, where the properties of the mixture are calculated as mole-fraction-weighed averages of the properties of the pure substances. The second one was the water – n-propanol system of the laboratory experiments, and it was chosen since both n-propanol and CO_2 are nonpolar, and thus the properties of the laboratory mixture were thought to mimic, at least qualitatively, the behaviour of the Martian system.

The possibilities for two-component nucleation were tested in two ways: first, the model browsed through the whole activity space using different temperatures. The model showed that two-component nucleation is possible in the whole parameter space. Second, the parameter space used in the model runs was limited to that valid in Martian near-surface conditions at the present epoch, as was done in the one-component nucleation studies of **Paper III**. Water concentrations from 1 ppm to 300 ppm were tested, and the mixture model was chosen to be ideal, since it is more favourable to

(a) (b)

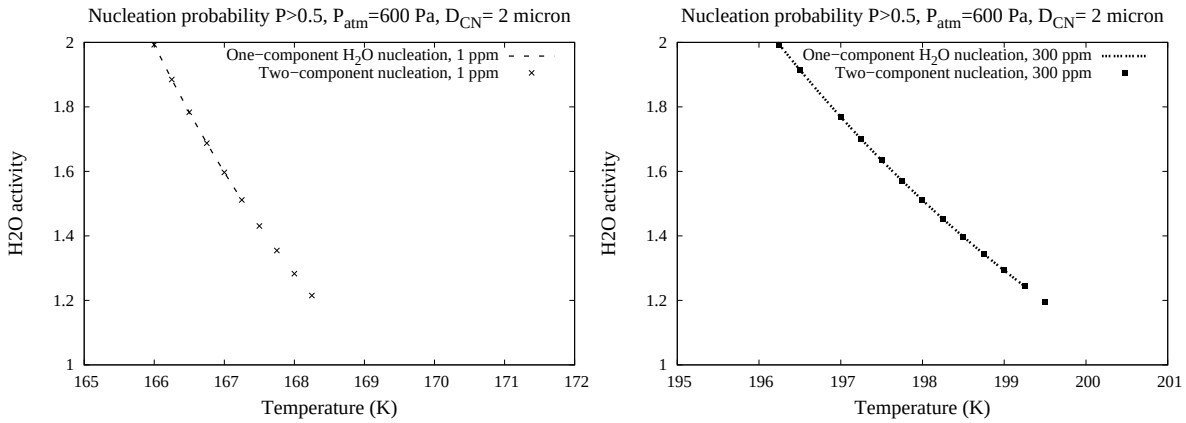

Figure 13: The critical activities of one- and two-component nucleation for P >0.5 as a function of temperature in the Martian case for (a) 1 ppm of water, and (b) 300 ppm of water. The lines describe one-component nucleation and the symbols two-component nucleation. The gas phase activity in one-component system is equivalent to the saturation ratio.

nucleation giving the lower limit of required activities. These model runs showed that assuming the ideal mixture approach, two-component nucleation can happen in the initial stages of one-component water nucleation, especially with small water amounts in the vapour phase (Figures 13a and b). The activities required for two-component nucleation are lower than those required for one-component nucleation. This result implies that near those conditions where the one-component water nucleation model predicts water nucleation, the two-component system nucleates as well, but it nucleates in slightly higher temperatures and lower activities than pure water. The amounts of molecules in the critical two-component cluster (Figure 14) show that with 1 ppm of water there are about 20 CO_2 molecules at maximum, and with 300 ppm the number of CO_2 molecules is smaller, about 2-3, mixed with some hundreds of water molecules in both cases. So the composition of the model-predicted clusters is clearly a mixture of CO_2 and H_2O. However, in this study several assumptions had to be made, especially related to the mixture properties, and since these properties affect nucleation onset very much, some data on the thermodynamic properties of the substances is required to confirm, or rule out, the results obtained here.

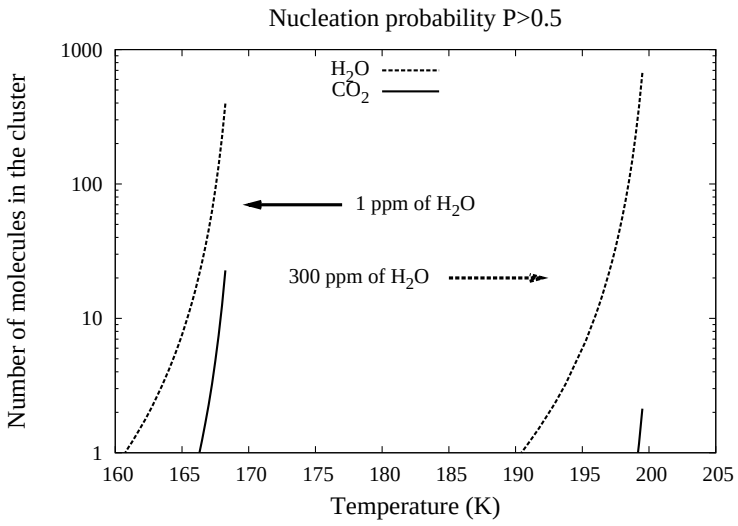

Figure 14: The number of molecules in the critical cluster as a function of temperature in the cases described in Figures 13a and b.

5 Remarks on models and the connection of the PBL and aerosols

5.1 Aerosols in the boundary layer

Important Martian aerosol processes occur near the surface. Dust is the radiatively dominant aerosol particle in the Martian atmosphere, and the source of dust is the surface. Dust is lifted to the atmosphere by a process called saltation, in which small sand grains are lifted by the wind, after which they hit the ground again, lifting smaller dust particles into the air. This process requires winds speeds reaching and overcoming a certain treshold of surface stress, and is thus largely dependent on the state of the near-surface atmosphere, the boundary layer. Since the prevailing (geostrophic) winds in the Martian near-surface environment often seem to be too weak to induce dust lifting, a possible answer to maintaining the background dustiness on Mars is the dust devils that frequently occur and exhibit magnitudes exceeding their Terrestrial analogs. The state of the PBL is dictating the formation of these vortices that are easily formed in strongly convective situations. As shown in Section 4, dust is a major atmospheric constituent affecting radiative transfer, and also cloud formation via the ability of dust particles to function as condensation nuclei (CN).

Ice crystals form via nucleation on dust particles during fog formation in the PBL, as shown in **Paper III**, and the fog formation was also modelled with a PBL model in **Papers I–II**. However, in the MPF investigations of **Papers I–III** daytime clouds do not form at the top of the boundary layer. There may be two reasons for this: First, the subtropical air is typically dry and thus low temperatures are required for cloud formation, and second, saturation is not reached in adiabatic cooling in ascending air because the diabatic term caused by the radiative warming effects of CO_2 and dust is dominating in the atmosphere during daytime. However, in other locations and seasons cloud formation in the boundary layer can be more frequent (for example in the polar night, see, e.g. Colaprete and Toon (2002)).

Ice crystals, when formed, can scavenge the dust they formed on from the atmosphere, since the crystals are bigger than dust particles, and thus have larger fall velocities. Thus cloud formation affects the dust distribution in two ways: First, cloud formation can limit the mixing of dust so that dust particles can not reach higher altitudes, since the dust particles are activated as CN in the area of cloud formation. Second, each cloud crystal cocoons a dust particle within, and takes it wherever they go, especially downwards via sedimentation, changing the vertical distribution of dust. The redistribution of dust and ice particles affects the thermal structure of the atmosphere, thus affecting cloud formation and mixing of dust. These aspects of water clouds on Mars have been looked into by Michelangeli et al. (1993) and Rodin et al. (1999). The system of feedbacks between turbulence, dust lifting, dust radiative effects, atmospheric

circulation and cloud formation is very complex, and detailed modeling and coupling of the components is required for accurate description of the atmospheric state.

5.2 Advantages and disadvantages of PBL and nucleation studies

The behaviour of the planetary boundary layer, despite the lack of exact theoretical understanding of turbulence, is well known through modeling and observational studies both on Earth and on Mars, and it has turned out that the similarity theory for turbulence can be used on both planets. Naturally data from the PBL of Mars is sparse: there are only three meteorological datasets, namely from VL1, VL2 and MPF, and some data from the mini-TES instruments of the MERs. The two time series from the Viking Landers covering more than 3 Martian years of data are still not fully analysed and call for more research on the structure of the PBL at different seasons.

Mesoscale (non-global) models extending from one to three dimensions are excellent testbeds because of their ability to model PBL processes with high resolution taking into account different mesoscale phenomena, like slope winds (2/3-D models), effect of contrasts in ice coverage or thermal properties of the soil (2/3-D), and even complex larger scale circulations (like baroclinic waves) via boundary conditions (3-D). Models can be developed to describe dust lifting, cloud formation, ice coverage on the surface and its changes, gravity waves, and other detailed phenomena. However, all the models need some input data. In the early days of modeling the Martian boundary layer (with only Viking Lander 1 and 2 observations) several assumptions had to be made in lack of data. For example, the roughness length of the surface (z_0) needed for boundary layer modeling had to be evaluated based on images sent by the landers: Haberle et al. (1993) used the estimation by Sutton et al. (1978). Information on the slope forcing at the lander sites had to be estimated as well (Haberle and Houben, 1991; Haberle et al., 1993), whereas nowadays the Martian surface has been mapped with high resolution by MOLA/MGS (Smith et al., 2001a) and information on slope angles and directions can be acquired. Even presently dust optical depth and water vapour amount have to be fit to observations from orbiting instruments for corresponding season unless the lander itself provides such measurements. For some models boundary conditions can not be acquired from observations only, but are needed from other models. Boundary conditions from a global climate model are crucial for a limited-area 3-D model, especially for longer climate simulations. For 1-D and 2-D models normally simpler boundary conditions are enough (prevailing average geostrophic wind, free-flow boundaries, etc.)

A 1-D model is an excellent tool for testing turbulence parameterizations and radiative transfer for Mars, since most of the lander data at hand are from locations and seasons without strong large scale disturbances (like baroclinic waves). Since in such

conditions and locations the largest influence comes from local turbulence and radiative effects, the model-produced temperature profiles compare well with observations. Winds produced by a 1-D model can be compared with observations in speed but not necessarily in direction, unless the landing site is completely flat, or slope effects are somehow included (as was done in Haberle and Houben, 1991; Haberle et al., 1993). A 1-D model is also computationally light and thus serves as a good testbed for testing parameterizations, which can then be used in larger scale models.

Naturally, all different scales are needed for atmospheric research, from the light 1-D models via mesoscale limited-area 3-D models to global climate models. All of them serve different purposes and thus complement each other. This continuity from small scale models all the way to global scale exists, and does not stop in 1-D in the smallest end, but goes all the way down to 0-D, implying, for example, a box model for cloud formation. Such models can be very precise and include all possible processes of influence, but they need input data from a larger model or observations. The 0-D models can be used for, for example, predicting cloud formation in any grid box in a large scale atmospheric model, or dust lifting and consequent processes at the surface or any atmospheric layer, and so forth, unless the computational expence becomes too high. These 0-D models are important for developing computationally lighter process parameterizations that can be included in large scale models, since often the full 0-D models are not computationally feasible to include in global scale models, or even in 3-D limited area models.

In this work I have focused on the smallest scales, 0-D and 1-D modeling of the Martian atmosphere, and especially on most accurate process description possible. The 0-D models developed and employed in this work are the one- and two-component nucleation models of **Papers III–V**, and in **Papers I–II** I used the 1-D model for Mars developed originally by Savijärvi (1991a,b). These studies can be used as a foundation for developing parameterizations of small scale phenomena in larger scale models. Naturally there are also drawbacks. The models can not self-consistently simulate the atmosphere, but need input data, and some processes are not described at all. The 0-D models for nucleation only describe particle formation, and not the consequent growth, so these models are only useful in calculating the initiation of cloud formation, but not the size of cloud particles, settling velocities, opacity of clouds, and so on. The detailed model results refine the large scale models via improvements in the process description, such as more accurate radiative transfer and critical saturation for cloud formation. For example, the computationally light one-component nucleation models can be included in large scale models and be used to calculate critical saturation ratios in different conditions (temperature, pressure, vapour amount, CN size). This has implications for cloud climatologies in global models. In radiative transfer schemes some aspects can be neglected (water vapour, ice clouds), but for instance in the northern summer near the north pole the water vapour amounts are large enough to have a significant effect on surface and near-surface temperatures, as shown by the 1-D model. Also in

studies of past Martian climate assuming a thicker CO_2 atmosphere leading to more CO_2 cloud formation, the radiative effects of clouds need to be taken into account for the climate modeling to be realistic. Thus the accurate models on smallest scales are vital for global climate studies by functioning as test benches for reviewing the scales of different processes and their overall importance among others.

6 Review of the papers

This thesis consists of five articles published in peer reviewed journals: one of the articles is a short technical note (**Paper IV**). All the papers deal with modeling the atmosphere of Mars with numerical models: only **Paper IV** has a weaker connection to Mars via comparison of results from **Paper III**. Two different approaches to study the Martian atmosphere have been adopted in the work presented in this thesis. The first two papers (**Papers I-II**) present results from studies of the boundary layer of Mars reflected via observations made by the Mars Pathfinder lander. The last three papers (**Papers III-V**) form a group of studies revolving around particle formation (nucleation) in the Martian atmosphere, utilizing classical nucleation theory applied to both one- and two-component nucleation. **Paper III** combines the two different regimes of the Martian atmosphere that are studied in this thesis by presenting results of particle formation in the planetary boundary layer of Mars.

- **Paper I** deals with one-dimensional model runs compared with the Mars Pathfinder data. The newly calibrated data had been received for comparison, and since the observations had changed, as well as the model radiative scheme, the model was compared against observations in a similar manner as in a previous investigation of the Mars Pathdinfer data (Savijärvi, 1999). This paper provides a baseline for the more detailed boundary-layer studies of **Paper II**.

- **Paper II** examines more in detail the boundary-layer processes at play in the Martian atmosphere, and especially the formulations used to describe them in the one-dimensional model. Emphasis is put on the treatment of turbulence and the effect different atmospheric constituents (CO_2, H_2O, dust) have on the radiative transfer. Surface temperature sensitivity was tested via different descriptions of the properties of the surface material, and results from a previous study (Mellon et al., 2000) were reproduced well. Tests were carried out to distinguish the relative roles of the soil thermal properties (thermal conductivity and heat capacity) in the surface temperature cycle. Also the conditions at the Beagle 2 landing site were predicted, but no data was received for comparison, since the lander was lost at landing.

- **Paper III** involves detailed theoretical investigation of one-component nucleation on Mars taking into account the effects of the condensation nuclei size, the approach for describing the growth of the formed embryo and the concentration of monomers of the system, and the non-isothermal effects for CO_2 on Mars. One-component nucleation models are developed for homogeneous and heterogeneous nucleation and for both components, CO_2 and H_2O. The results of the CO_2 model are compared also against laboratory measurements, and those of the water model against previous modeling results.

- **Paper IV** provides mainly a more accurate description of theory of nucleation used in **Paper III**, and compares the results using the old and the new approach. This is also the first publication of the exact form of the one-component heterogeneous Zeldovich factor for spherical particles in the literature.

- **Paper V** introduces a completely new approach to nucleation on Mars, the concept of two-component nucleation. A two-component homogeneous nucleation model utilizing the exact Stauffer kinetics is modified for heterogeneous nucleation, and tested against laboratory experiments. Also two approximate approaches for nucleation kinetics are tested. After testing the model it is used to investigate the possibility of two-component nucleation of the Martian binary system of CO_2 and H_2O.

Author's contribution

I am alone responsible for the summary of the thesis.

In **Paper I** I was responsible for the numerical calculations. I collaborated in writing all parts of the article.

In **Paper II** I carried out the numerical calculations for the sensitivity tests. I also retrieved all the required parameters for the Beagle 2 model runs and and performed them. I wrote the main bulk of the article.

For **Paper III** I developed models for calculating nucleation rates of one-component homogeneous nucleation and heterogeneous nucleation on spherical surfaces and applied them to the Martian conditions. I made all the numerical calculations and I also wrote nearly completely all the sections of the paper.

The **Paper IV** presents the accurate formulation of the heterogeneous Zeldovich factor derived by H. Vehkamäki: my role in this paper has been the initiator of more detailed heterogeneous nucleation studies that have lead to the derivation of the accurate form. I also conducted the numerical calculations and the comparison that are presented in this paper: it improves the model described in **Paper III** and is thus linked to my own work. I also wrote the result section of the paper and participated in writing the other sections.

In **Paper V** I carried out the main modifications required to the model when dealing with heterogeneous nucleation, and conducted the model runs. The main body of the paper is written mainly by myself, with the exception of the theory of binary nucleation and the Appendix A.

7 Summary and future prospects

The driving force of the work in this thesis has been the awareness of several still unanswered questions in Mars meteorology and climatology. Although the planet has been observed with detailed instruments for decades, the scientific community is still faced with surprises and puzzling observations. However, also Mars atmospheric models have been developed for decades, ranging from global 3-D models to very local, 1-D column models, or even 0-D cloud models, and with the help of models and observations to constrain them, the present Martian climate is fairly well known.

My interest in the work conducted during this thesis has mostly been the development of process description already in use in atmospheric models, such as turbulence, radiation, and cloud formation. In particular, testing for two-component nucleation has been the first attempt to model this phenomenon in Martian conditions, and the quite theoretical results can be seen interesting and calling for more research on the topic. Overall my playfield in the framework of research of the Martian atmosphere has been in zooming up certain processes and looking into them in detail.

The main results of this thesis are the following:

- Turbulence in the Martian PBL can be described with the help of similarity theory and stability functions used for the Terrestrial PBL.
- Water vapour, along with dust, has a large impact on the downwelling longwave radiation, which affects the surface temperatures significantly, especially during nighttime. Thus water vapour should be included in Mars atmospheric models as an important and very variable greenhouse gas.
- The turbulent surface heat fluxes on Mars are so small in the diurnal thermal evolution of the soil that they can be left out when, for example, deriving thermal inertia values from satellite observations.
- Cloud formation on Mars takes place in a majority of cases via heterogeneous nucleation on the ubiquitous dust suspended in the atmosphere.
- The critical saturation ratios required for cloud formation clearly exceed unity for both CO_2 and H_2O clouds. Thus, for correct cloud climatologies in atmospheric models the critical conditions for cloud formation should be calculated correctly instead of assuming cloud formation to start at $S = 1$.
- Two-component nucleation on Mars is theoretically possible at nearly the same conditions as one-component water nucleation (assuming ideal mixture).

Observations are an important part of research, and in my opinion one of the most important goals of future missions would be to get meteorological instrument packages onboard every lander headed for Mars. The next big step in Mars atmospheric research would be a network mission with meteorological equipment, as planned in the MetNet project. However, support for such projects from the whole Mars science community would be needed instead of them being left in the margins of focus. Fortunately, the ExoMars and NEXT projects of the European Space Agency have a framework enabling network missions. For meteorological purposes observations from anywhere on the planet are useful: also the Earth's continents are covered with weather stations and ships provide data from the seas. Such continuous observations are vital for terrestrial weather prediction models and meteorologists using them: the meteorologists who make the final weather predictions refine, based on the newest observations, the computer-predicted fields that use older observational data. For atmospheric research on Mars to go up to the next level, we need to aim towards continuous weather data enabling forecasting efforts. Through this approach also Martian climate studies can be pushed forward via understanding of present mesoscale phenomena, like local dust storms and dust lifting in general, cloud formation, and so forth, since these processes play a significant role in the climate. Considering dust and ice crystals, we still do not know enough of their composition, size distributions and scattering properties. An instrument designed to measure the size distribution of dust and its composition would come in handy at this stage when the models are already so accurate that we need to know the smallest details very well, particularly considering the radiative transfer, which is so important in the dusty climate. The radiative effect of the clouds is small, but for model validation some knowledge on the crystal composition, shapes, and size distributions would be needed. Remote sensing can give us quite good evaluations, but at least some measurements inside a radiative surface fog would be necessary. Infrared spectroscopy of ice crystals could help us distinguish if there really are conditions where CO_2 and H_2O condense together and/or form clathrate, on the ground or in the atmosphere.

In addition to acquiring more observations, both in amount and in accuracy, models and the theoretical background need to be improved constantly. This thesis has pushed forward some aspects, but there are still points to be addressed in the topics covered by my research summarized here. Scientific research is an iterative process, and thus this thesis is merely one step forward in that continuing path.

References

Alestalo, M. and Savijärvi, H.: Mesoscale circulations in a hydrostatic model: coastal convergence and orographic lifting, Tellus, 37A, 156–162, 1985.

Alpert, P., Cohen, A., Neumann, J., and Doron, E.: A model simulation of the summer circulation from the eastern Mediterranean past Lake Kinneret in the Jordan valley, Mon. Wea. Rev., 110, 994–1006, 1982.

Arya, S. P.: Introduction to Micrometeorology, Academic Press, San Diego, 307 s., 1988.

Basu, S., Wilson, J., Richardson, M., and Ingersoll, A.: Simulation of spontaneous and variable global dust storms with the GFDL Mars GCM, J. Geophys. Res., 111, E09 004, doi:10.1029/2005JE002660, 2006.

Benson, J. L., James, P. B., Cantor, B. A., and Remigio, R.: Interannual variability of water ice clouds over major martian volcanoes observed by MOC, Icarus, 184, 365–371, 2006.

Bertaux, J.-L., Fonteyn, D., Korablev, O., Chassefiere, E., Dimarellis, E., Dubois, J. P., Hauchecorne, A., Cabane, M., Rannou, P., Levasseur-Regourd, A. C., Cernogora, G., Quemerais, E., Hermans, C., Kockarts, G., Lippens, C., Maziere, M. D., Moreau, D., Muller, C., Neefs, B., Simon, P. C., Forget, F., Hourdin, F., Talagrand, O., Moroz, V. I., Rodin, A., Sandel, B., and Stern, A.: The study of the Martian atmosphere from top to bottom with SPICAM light on Mars Express, Planet. Space Sci., 48, 1303–1320, 2000.

Bibring, J.-P., Langevin, Y., Poulet, F., Gendrin, A., Gondet, B., Berthe, M., Soufflot, A., Drossart, P., Combes, M., Bellucci, G., moroz, V., Mangold, N., Schmitt, B., and the OMEGA team: Perennial water ice identified in the south polar cap of Mars, Nature, 428, 627–630, 2004a.

Bibring, J.-P., Soufflot, A., Berthe, M., Langevin, Y., Gondet, B., Drossart, P., Bouye, M., Combes, M., Puget, P., Semery, A., Bellucci, G., Formisano, V., Moroz, V., Kottsov, V., the OMEGA Co-I team, Bonello, G., Erard, S., Forni, O., Gendrin, A., Manaud, N., Poulet, F., Poulleau, G., Encrenaz, T., Fouchet, T., Melchiorri, R., Altieri, F., Ignatiev, N., Titov, D., Zasova, L., Coradini, A., Capacionni, F., Cerroni, P., Fonti, S., Mangold, N., Pinet, P., Schmitt, B., Sotin, C., Hauber, E., Hoffmann, H., Jaumann, R., Keller, U., Arvidson, R., Mustard, J., and Forget, F.: OMEGA: Observatoire pour la minéralogie, l'eau, les glaces et l'activité, ESA SP-1240: Mars Express: the scientific payload, pp. 37–49, 2004b.

Bingham, S. J., Lewis, S. R., Newman, C. E., and Read, P. L.: Environmental predictions for the Beagle 2 lander, based on GCM climate simulations, Planet. Space Sci., 52, 259–269, 2004.

Böttger, H. M., Lewis, S. R., Read, P. L., and Forget, F.: The effects of Martian regolith on GCM water cycle simulations, Icarus, 177, 174–189, 2005.

Boynton, W. V., Feldman, W. C., Squyres, S. W., Prettyman, T. H., Brückner, J., Evans, L. G., Reedy, R. C., Starr, R., Arnold, J. R., Drake, D. M., Englert, P. A. J., Metzger, A. E., Mitrofanov, I., Trombka, J. I., d'Uston, C., Wänke, H., Gasnault, O., Hamara, D. K., Janes, D. M., Marcialis, R. L., Maurice, S., Mikheeva, I., Taylor, G. J., Tokar, R., and Shinohara, C.: Distribution of hydrogen in the near surface of Mars: evidence for subsurface ice deposits, Science, 297, 81–85, doi:10.1126/science.1073722, 2002.

Briggs, G., Klaasen, K., Thorpe, T., and Wellman, J.: Martian Dynamical Phenomena During June-November 1967: Viking Orbiter Imaging Results, J. Geophys. Res., 82, 4121–4149, 1977.

Cantor, B. A., James, P. B., Caplinger, M., and Wolff, M. J.: Martian dust storms: 1999 Mars Orbiter Camera observations, J. Geophys. Res., 106, 23 653–23 687, 2001.

Christensen, P. R., Banfield, J. L., Hamilton, V. E., Ruff, S. W., Kieffer, H. H., Titus, T. N., Malin, M. C., Morris, R. V., Lane, M. D., Clark, R. L., Jakosky, B. M., Mellon, M. T., Pearl, J. C., Conrath, B. J., Smith, M. D., Clancy, R. T., Kuzmin, R. O., Roush, T., Mehall, G. L., Gorelick, N., Bender, K., Murray, K., Dason, S., Greene, E., Silverman, S., and Greenfield, M.: Mars Global Surveyor Thermal Emission Spectrometer experiment: Investigation description and surface science results, J. Geophys. Res., 106, 23 823–23 872, 2001.

Clancy, R. I., Grossman, A. W., Wolff, M. J., James, P. B., Rudy, D. J., Billawala, Y. N., Sandor, B. J., Lee, S. W., and Muhleman, D. O.: Water Vapor Saturation at Low Altitudes around Mars Aphelion: A Key to Mars Climate?, Icarus, 122, 36–62, 1996.

Clancy, R. T. and Sandor, B. J.: CO_2 ice clouds in the upper atmosphere of Mars, Geophys. Res. Lett., 25, 489–492, 1998.

Clancy, R. T., Wolff, M. J., and Christensen, P. R.: Mars aerosol studies with the MGS TES emission phase function observations: Optical depths, particles sizes, and ice cloud types versus latitude and solar longitude, J. Geophys. Res., 108, 5098, doi:10.1029/2003JE002058, 2003.

Clancy, R. T., Wolff, M. J., Whitney, B. A., Cantor, B. A., and Smith, M. D.: Mars equatorial mesospheric clouds: Global occurrence and physical properties from Mars Global Surveyor Thermal Emission Spectrometer and Mars Orbiter Camera limb observations, J. Geophys. Res., 112, E04 004, doi:10.1029/2006JE002805, 2007.

Colaprete, A. and Toon, O. B.: Carbon dioxide snow storms during the polar night on Mars, J. Geophys. Res., 107, 2002.

Colaprete, A. and Toon, O. B.: Carbon dioxide clouds in an early dense Martian atmosphere, J. Geophys. Res., 108, 2003.

Colaprete, A., Toon, O. B., and Magalhaes, J. A.: Cloud formation under Mars Pathfinder conditions, J. Geophys. Res., 104, 1999.

Colaprete, A., Haberle, R. M., and Toon, O. B.: Formation of convective carbon dioxide clouds near the south pole of Mars, J. Geophys. Res., 108, 2003.

Delage, Y. and Girard, C.: Stability functions correct at the free convection limit and consistent for both the surface and Ekman layers, Boundary-Layer Meteorol., 58, 19–31, 1992.

Desjean, M. C., Forget, F., and Lopez-Valverde, M., eds.: Proceedings of the Second International Workshop on Mars atmosphere modelling and observations, Centre national d'etudes spatiales, European Space Agency, Instituto de astrofisica de Andalucia, Laboratoire de meteorologie dynamique / Centre national de recherches scientifiques, University of Oxford, 2006.

Douté, S., Schmitt, B., Langevin, Y., Bibring, J.-P., Altieri, F., Bellucci, G., Gondet, B., Poulet, F., and the MEX OMEGA team: South Pole of Mars: Nature and composition of the icy terrains from Mars Express OMEGA observations, Planet. Space Sci., 55, 113–133, 2007.

Dyer, A. J.: A review of the flux profile relationships, Boundary-Layer Meteorol., 7, 363–372, 1974.

Encrenaz, T., Fouchet, T., Melchiorri, R., Drossart, P., Gondet, B., Langevin, Y., Bibring, J.-P., Forget, F., and Bezard, B.: Seasonal variations of the Martian CO over Hellas as observed by OMEGA/Mars Express, Astron. and Astrophys., 459, 265–270, 2006.

Fanale, F. P., Postawko, S. E., Pollack, J. B., Carr, M. H., and Pepin, R. O.: Mars: epochal climate change and volatile history, in: Kieffer et al. (1992), pp. 1135–1179, 1992.

Feder, J., C., R. K., Lothe, J., and Pound, G. M.: Homogeneous Nucleation and Growth of Droplets in Vapours, Advances in Physics, 15, 111–178, 1966.

Fedorova, A. A., Lellouch, E., Titov, D. V., de Graauw, T., and Feuchtgruber, H.: Remote sounding of the Martian dust from ISO spectroscopy in the 2.7 μm CO_2 bands, Planet. Space Sci., 50, 3–9, 2002.

Fenton, L. K., Geissler, P. E., and Haberle, R. M.: Global warming and climate forcing by recent albedo changes on Mars, Nature, 446, 646–649, doi:10.1038/nature05718, 2007.

Fergason, R. L., Christensen, P. R., and Kieffer, H. H.: High-resolution thermal inertia derived from the Thermal Emission Imaging System (THEMIS): Thermal model and applications, J. Geophys. Res., 111, E12 004, doi:10.1029/2006JE002735, 2006.

Fletcher, N.: Size effect in heterogeneous nucleation, J. Chem. Phys, 29, 572–576, 1958.

Forget, F.: Improved optical properties of the Martian atmospheric dust for radiative transfer calculations in the infrared, Geophys. Res. Lett., 25, 1105–1108, 1998.

Forget, F. and Pierrehumbert, R. T.: Warming early Mars with carbon dioxide clouds that scatter infrared radiation, Science, 278, 1273–1276, 1997.

Forget, F., Spiga, A., Dolla, B., Vinatier, S., Melchiorri, R., Drossart, P., Gendrin, A., Bibring, J.-P., Langevin, Y., and Gondet, B.: Remote sensing of surface pressure on Mars with the Mars Express/OMEGA spectrometer: 1. Retrieval method, J. Geophys. Res., 112, E08S15, doi:10.1029/2006JE002871, 2007.

Formisano, V., Angrilli, F., Arnold, G., Atreya, S., Bianchini, G., Biondi, D., Blanco, A., Bleka, M. I., Coradini, A., Colangeli, L., Ekonomov, A., Encrenaz, T., Esposito, F., Fonti, S., Giuranna, M., Grassi, D., Gnedykh, V., Grigoriev, A., Hansen, G., Hirsh, H., Khatuntsev, I., Kiselev, A., Ignatiev, N., Jurewicz, A., Lellouch, E., Moreno, J. L., Marten, A., Mattana, A., Maturilli, A., Mencarelli, E., Michalska, M., Moroz, V., Moshkin, B., Nespoli, F., Nikolsky, Y., Orfei, R., Orleanski, P., Orofino, V., Palomba, E., Patsaev, D., Piccioni, G., Rataj, M., Rodrigo, R., Rodriguez, J., Rossi, M., Saggin, B., Titov, D., and Zasova, L.: The Planetary Fourier Spectrometer (PFS) onboard the European Mars Express mission, Planet. Space Sci., 53, 963–974, 2005.

Fuerstenau, S. D.: Solar heating of suspended particles and the dynamics of Martian dust devils, Geophys. Res. Lett., 33, L19S03, doi:10.1029/2006GL026798, 2006.

Galvéz, O., Ortega, I. K., Maté, B., Moreno, M. A., Martín-Llorente, B., Herrero, V. J., Escribano, R., and Gutiérrez, P. J.: A study of the intercation of CO_2 with water ice, Astron. and Astrophys., 472, 691–698, 10.1051/0004-6361:20077421, 2007.

Garcia-Comas, M., Keller, H. U., Titov, D. V., Maltagliati, L., Inada, A., and Bibring, J.-P.: OMEGA spot pointing observations of Mars aerosols, in: Desjean et al. (2006), p. 2.2.2., 2006.

Glandorf, D. L., Colaprete, A., Tolbert, M. A., and Toon, O. B.: CO_2 Snow on Mars and Early Earth: Experimental Constraints, Icarus, 160, 66–72, 2002.

Golombek, M. P. I., Jr., N. T. B., Moore, H. J., Murchie, S. L., Murphy, J. R., Parker, T. J., Rieder, R., Rivellini, T. P., Schofield, J. T., Seiff, A., Singer, R. B., Smith, P. H., Soderblom, L. A., Spencer, D. A., Stoker, C. R., Sullivan, R., Thomas, N., Thurman, S. W., Tomasko, M. G., Vaughan, R. M., Wänke, H., Ward, A. W., and

Wilson, G. R.: Overview of the Mars Pathfinder Mission: Launch through landing, surface operations, data sets, and science results, J. Geophys. Res., 104, 8523–8554, 1999.

Gooding, J. L.: Martian dust particles as condensation nuclei: A preliminary assesment of mineralogical factors, Icarus, 66, 56–74, 1986.

Greeley, R.: Saltation impact as a means for raising dust on Mars, Planet. Space Sci., 50, 151–155, 2002.

Greeley, R., Balme, M. P., Iversen, J. D., Metzger, S., Mickelson, R., Phoreman, J., and White, B.: Martian dust devils: Laboratory simulations of particle threshold, J. Geophys. Res., 108, 5041, doi:10.1029/2002JE001987, 2003.

Haberle, R. M. and Houben, H. C.: Mars boundary layer simulations: comparison with Viking lander and entry observation, in: The Environmental Model of Mars, pp. 3–6, 1991.

Haberle, R. M., Houben, H. C., Hertenstein, R., and Herdtle, T.: A boundary-layer model for Mars: comparison with Viking Lander and entry data, J. Atmos. Sci., 50, 1544–1559, 1993.

Haberle, R. M., Barnes, J. R., Murphy, J. R., Joshi, M. M., and Schaeffer, J.: Meteorological predictions for the Mars Pathfinder lander, J. Geophys. Res., 102, 13 301–13 311, 1997.

Haberle, R. M., McKay, C. P., Schaeffer, J., Cabrol, N. A., Grin, E. A., Zent, A. P., and Quinn, R.: On the possibility of liquid water on present-day Mars, J. Geophys. Res., 106, 23 317–23 326, 2001.

Harri, A.-M., Marsal, O., Lognonne, P., Leppelmeier, G. W., Spohn, T., Glassmeier, K.-H., Angrilli, F., Banerdt, W. B., Barriot, J. P., Bertaux, J.-L., Berthelier, J. J., Calcutt, S., Cerisier, J. C., Crisp, D., Dehant, V., Giardini, D., Jaumann, R., Langevin, Y., Menvielle, M., Mussmann, G., Pommereau, J. P., di Pippo, S., Guerrier, D., Kumpulainen, K., Larsen, S., Mocquet, A., Polkko, J., Runavot, J., Schumacher, W., Siili, T., Simola, J., Tillman, J. E., and the NetLander Team: Network science landers for Mars, Adv. Space Res., 23, 1915–1924, 1999.

Harri, A.-M., Makkonen, P., Polkko, J., Lappalainen, H., Pellinen, R., Vorontsov, V., Polyakov, A., Ivankov, A., Linkin, V., Gotlib, V., and Lipatov, A.: METNET — the next generation lander for Martian atmospheric science, in: Proceedings of the 54th International Astronautical Congress, IAC-03-Q.3.b.09, 2003.

Hecht, M. H.: Metastability of liquid water on Mars, Icarus, 156, 373–386, doi:10.1006/icar.2001.6794, 2002.

Hess, S. L., Henry, R. M., Leovy, C. B., Mitchell, J. L., Ryan, J. A., and Tillman, J. E.: Early Meteorological Results from the Viking 2 Lander, Science, 194, 1352–1353, 1976.

Hess, S. L., Henry, R. M., Leovy, C. B., Ryan, J. A., and Tillman, J. E.: Meteorological results from the surface of Mars: Viking 1 and 2, J. Geophys. Res., 82, 4559–4574, 1977.

Houghton, J., Ding, Y., Griggs, D., Noguer, M., van der Linden, P., Dai, X., Maskell, K., and Johnson, C., eds.: Climate Change 2001: The Scientific Basis. Contribution of Working Group I to the Third Assessment Report of the Intergovernmental Panel on Climate Change, Cambridge University Press, Cambridge, United Kingdom and New York, NY, USA, 881 pp., 2001.

Hunt, G. E. and James, P. B.: Martian extratropical cyclones, Nature, 278, 531–532, 1979.

Hunt, G. E. and James, P. B.: Martian cloud systems: current knowledge and future observations, Adv. Space Res., 5, 93–99, 1985.

Hunt, G. E., Pickersgill, A. O., James, P. B., and Evans, N.: Daily and seasonal Viking observations of Martian bore wave systems, Nature, 293, 630–633, 1981.

Inada, A.: Simulations of Martian surface fog and calibration of Mars Imaging Camera for its future observations, Ph.D. thesis, Kobe University, Japan, 2002.

Ivanov, A. B. and Muhleman, D. O.: Cloud Reflection Observations: Results from the Mars Orbiter Laser Altimeter, Icarus, 154, 190–206, 2001.

Jakosky, B. M.: Out on a limb: Martian atmospheric dust opacity during the past hundred years, Icarus, 117, 1995.

Jakosky, B. M. and Farmer, C. B.: The seasonal and global behavior of water vapor in the Mars atmosphere: complete global results of the Viking atmospheric water detector experiment, J. Geophys. Res., 87, 2999–3019, 1982.

Jakosky, B. M., Mellon, M. T., Kieffer, H. H., Christensen, P. R., Varnes, E. S., and Lee, S. W.: The thermal inertia of Mars from the Mars Global Surveyor Thermal Emission Spectrometer, J. Geophys. Res., 105, 9643–9652, 2000.

James, P. B., Kieffer, H. H., and Paige, D. A.: The seasonal cycle of carbon dioxide on Mars, in: Kieffer et al. (1992), pp. 934–968, 1992.

Kahn, R.: The spatial and seasonal distribution of Martian clouds and some meteorological implications, J. Geophys. Res., 89, 6671–6688, 1984.

Kahn, R. and Gierasch, P.: Long cloud observations on Mars and implications for boundary layer characteristics over slopes, J. Geophys. Res., 87, 867–880, 1982.

Kanak, K. M.: On the numerical simulation of dust devil-like vortices in Terrestrial and Martian convective boundary layers, Geophys. Res. Lett., 33, L10S05, doi:10.1029/2006GL026207, 2006.

Kasting, J. F.: CO_2 Condensation and the Climate of Early Mars, Icarus, 94, 1–13, 1991.

Keesee, R. G.: Nucleation and particle formation in the upper atmosphere, J. Geophys. Res., 94, 14 683–14 692, 1989.

Kieffer, H. H. and Zent, A. P.: Quasi-periodic climate change on Mars, in: Kieffer et al. (1992), pp. 1180–1218, 1992.

Kieffer, H. H., Chase, S. C., Miner, E. D., Palluconi, F. D., Munch, G., Neugebauer, G., and Martin, T. Z.: Infrared thermal mapping of the Martian surface and atmosphere: first results, J. Geophys. Res., 82, 4249–4291, 1976.

Kieffer, H. H., Martin, T. Z., Peterfreund, A. R., Jakosky, B. M., Miner, E. D., and Palluconi, F. D.: Thermal and albedo mapping of Mars during the Viking primary mission, J. Geophys. Res., 82, 4249–4291, 1977.

Kieffer, H. H., Jakosky, B. M., Snyder, C. W., and Matthews, M. S., eds.: Mars, University of Arizona Press, 1992.

Kulmala, M., Lauri, A., Vehkamäki, H., Laaksonen, A., Petersen, D., and Wagner, P. E.: Strange predictions by binary heterogeneous nucleation theory compared with a quantitative experiment, J. Phys. Chem. B., 105, 11 800–11 808, 2001.

Kulmala, M., Lehtinen, K. E. J., and Laaksonen, A.: Cluster activation theory as an explanation of the linear dependence between formation rate of 3 nm particles and sulphuric acid concentration, Atmos. Chem. Phys., 6, 787–793, 2006.

Kurgansky, M. V.: Steady-state properties and statistical distribution of atmospheric dust devils, Geophys. Res. Lett., 33, L19S06, doi:10.1029/2006GL026142, 2006.

Langevin, Y., Poulet, F., Bibring, J.-P., Schmitt, B., Doute, S., and Gondet, B.: Summer evolution of the north polar cap of Mars as observed by OMEGA/Mars Express, Science, 307, 1581–1584, 2005.

Larsen, S. E., Jorgensen, H. E., Landberg, L., and Tillman, J. E.: Aspects of the atmospheric surface layers on Mars and Earth, Boundary-Layer Meteorol., 105, 451–470, 2002.

Lazaridis, M., Kulmala, M., and Gorbunov, B. Z.: Binary heterogeneous nucleation at a non-uniform surface, J. Aerosol Sci., 23, 457–466, 1992.

Lebonnois, S., Quemerais, E., Montmessin, F., Lefevre, F., Perrier, S., Bertaux, J.-L., and Forget, F.: Vertical distribution of ozone on Mars as measured by SPICAM/Mars Express using stellar occultation, J. Geophys. Res., 111, E09S05, doi:10.1029/2005JE002643, 2006.

Lemmon, M. T., Wolff, M. J., Smith, M. D., Clancy, R. T., Banfield, D., Landis, G. A., Ghosh, A., Smith, P. H., Spanovich, N., Whitney, B., Whelley, P., Greeley, R., Thompson, S., Bell, III, J. F., and Squyres, S. W.: Atmospheric imaging results from the Mars Exploration Rovers: Spirit and Opportunity, Science, 306, 1753–1756, 2004.

Levrard, B., Forget, F., Montmessin, F., and Laskar, J.: Recent formation and evolution of northern Martian polar layered deposits as inferred from a Global Climate Model, J. Geophys. Res, 112, E06 012, doi:10.1029/2006JE002772, 2007.

Lewis, S. R., Collins, M., Read, P. L., Forget, F., Hourdin, F., Fournier, R., Hourdin, C., Talagrand, O., and Huot, J.-P.: A climate database for Mars, J. Geophys. Res., 104, 24 177–24 194, 1999.

Longhi, J.: Phase equilibrium in the system CO_2–H_2O: application to Mars, J. Geophys. Res., 111, doi:10.1029/2005JE002552, 2006.

Määttänen, A., Fouchet, T., Drossart, P., Melchiorri, R., Encrenaz, T., Combes, M., Bibring, J.-P., Langevin, Y., Gondet, B., Poulet, F., Titov, D. V., and the OMEGA team: Constraining the Martian dust properties from the Mars Express/OMEGA data, in: Desjean et al. (2006), p. 2.2.6, 2006.

Magalhaes, J. A., Schofield, J. T., and Seiff, A.: Results of the Mars Pathfinder atmospheric structure investigation, J. Geophys. Res., 104, 8943–8955, 1999.

Martin, L. and Zurek, R.: An analysis of the history of dust activity on Mars, J. Geophys. Res., 98, 3221–3246, 1993.

Martin, L. J., James, P. B., Dollfus, A., Iwasaki, K., and Beish, J. D.: Telescopic observations: visual, photographic, polarimetric, in: Kieffer et al. (1992), pp. 34–70, 1992.

McCleese, D. J., Schofield, J. T., Taylor, F. W., Calcutt, S. B., Foote, M. C., kass, D. M., Leovy, C. B., Paige, D. A., Read, P. L., and Zurek, R. W.: Mars Climate Sounder: An investigation of thermal and water vapor structure, dust and condensate distributions in the atmosphere, and energy balance of the polar regions, J. Geophys. Res., 112, E05S06, doi:10.1029/2006JE002790, 2007.

McCord, T. B., Adams, J. B., Bellucci, G., Combe, J.-P., Gillespie, A. R., Hansen, G., Hoffmann, H., Jaumann, R., Neukum, G., Pinet, P., Poulet, F., and Stephan, K.: Mars Express High Resolution Stereo Camera spetrophotometric data: Characteristics and science analysis, J. Geophys. Res., 112, E06 004, doi:10.1029/2006JE002769, 2007.

McEwen, A. S., Eliason, E. M., Bergstrom, J. W., Bridges, N. T., Hansen, C. J., Delamere, W. A., Grant, J. A., Gulick, V. C., Herkenhoff, K. E., Keszthelyi, L., Kirk, R. L., Mellon, M. T., Squyres, S. W., Thomas, N., and Weitz, C. M.: Mars Reconnaissance Orbiter's High Resolution Imaging Science Experiment (HiRISE), J. Geophys. Res., 112, E05S02, doi:10.1029/2005JE002605, 2007.

Melchiorri, R., Drossart, P., Fouchet, T., Vinatier, S., Forget, F., Bellucci, G., Altieri, F., Bibring, J.-P., Langevin, Y., and Manaud, N.: Atmospheric waves from OMEGA/Mars Express data, in: Geophysical Research Abstracts, vol. 7, p. 08375, European Geosciences Union, 2005.

Melchiorri, R., Drossart, P., Fouchet, T., Bezard, B., Forget, F., Gendrin, A., Bibring, J.-P., Manaud, N., and team, O.: A simulation of the OMEGA/Mars Express observations: analysis of the atmospheric contribution, Planet. Space Sci., 54, 774–783, 2006.

Melchiorri, R., Encrenaz, T., Fouchet, T., Drossart, P., Lellouch, E., Gondet, B., Bibring, J.-P., Langevin, Y., Schmitt, B., Titov, D., and Ignatiev, N.: Water vapor mapping on Mars using OMEGA/Mars Express, Planet. Space Sci., 55, 333–342, 2007.

Mellon, M. T., Jakosky, B. M., Kieffer, H. H., and Christensen, P. R.: High-resolution thermal inertia mapping from the Mars Global Surveyor Thermal Emission spectrometer, Icarus, 148, 437–455, 2000.

Merikallio, S.: Available Solar Energy on the Dusty Martian Atmosphere and Surface, M.Sc. thesis (tech.), Helsinki University of Technology, 2003.

Metzger, S. M., Carr, J. R., Johnson, J. R., Parker, T. J., and Lemmon, M.: Dust devil vortices seen by the Mars Pathfinder camera, Geophys. Res. Lett., 26, 2781–2784, 1999.

Michaels, T. I.: Numerical modeling of Mars dust devils: Albedo track generation, Geophys. Res. Lett., 33, L19S08, doi:10.1029/2006GL026268, 2006.

Michaels, T. I., Colaprete, A., and Rafkin, S. C. R.: Significant vertical water transport by mountain-induced circulations on Mars, Geophys. Res. Lett., 33, L16 201, doi:10.1029/2006GL026562, 2006.

Michelangeli, D. V., Toon, O. B., Haberle, R. M., and Pollack, J. B.: Numerical simulations of the formation and evolution of water ice clouds in the Martian atmosphere, Icarus, 100, 261–285, 1993.

Montmessin, F., Bertaux, J.-L., Quemerais, E., Korablev, O., Rannou, P., Forget, F., Perrier, S., Fussen, D., Lebonnois, S., Reberac, A., and Dimarellis, E.: Subvisible CO_2 clouds detected in the mesosphere of Mars, Icarus, 183, 403–410, 2006a.

Montmessin, F., Gondet, B., Fouchet, T., Drossart, P., Bibring, J.-P., Bertaux, J.-L., and Langevin, Y.: Spectroscopic detection of low latitudes carbon dioxide clouds in the middle atmosphere of Mars, in: American Geophysical Union, Fall Meeting 2006, abstract P14A-03, 2006b.

Montmessin, F., Quémerais, E., Bertaux, J.-L., Korablev, O., Rannou, P., and Lebonnois, S.: Stellar occultations at UV wavelengths by the SPICAM instrument: Retrieval and analysis of Martian haze profiles, J. Geophys. Res., 111, E09S09, doi:10.1029/2005JE002662, 2006c.

Montmessin, F., Gondet, B., Bibring, J.-P., Langevin, Y., Drossart, P., Forget, F., and Fouchet, T.: Hyper-spectral imaging of convective CO_2 ice clouds in the equatorial mesosphere of Mars, J. Geophys. Res., 112, doi:10.1029/2007JE002944, in print, 2007a.

Montmessin, F., Haberle, R. M., Forget, F., Langevin, Y., Clancy, R. T., and Bibring, J.-P.: On the origin of perennial water ice at the south pole of Mars: A precession-controlled mechanism?, J. Geophys. Res., 112, E08S17, doi:10.1029/2007JE002902, 2007b.

Murchie, S., Arvidson, R., Bedini, P., Beisser, K., Bibring, J.-P., Bishop, J., Boldt, J., Cavender, P., Choo, T., Clancy, R. T., Darlington, E. H., Marais, D. D., Espiritu, R., Fort, D., Green, R., Guinness, E., Hayes, J., Hash, C., Heffernan, K., Hemmler, J., Heyler, G., Humm, D., Hutcheson, J., Izenberg, N., Lee, R., Lees, J., Lohr, D., Malaret, E., Martin, T., McGovern, J. A., McGuire, P., Morris, R., Mustard, J., Pelkey, S., Rhodes, E., Robinson, M., Roush, T., Schaefer, E., Seagrave, G., Seelos, F., Silverglate, P., Slavney, S., Smith, M., Shyong, W.-J., Strohbehn, K., Taylor, H., Thompson, P., Tossman, B., Wirzburger, M., and Wolff, M.: Compact Reconnaissance Imaging Spectrometer for Mars CRISM on Mars Reconnaissance Orbiter (MRO), J. Geophys. Res., 112, E05S03, doi:10.1029/2006JE002682, 2007.

Murphy, J. R., Pollack, J. B., Haberle, R. M., Leovy, C. B., Toon, O. B., and Schaeffer, J.: Three-dimensional numerical simulation of Martian dust storms, J. Geophys. Res., 100, 26 357–26 376, 1995.

Neukum, G., Jaumann, R., and the HRSC Co-Investigator and Experiment Team: HRSC: the high resolution stereo camera of Mars Express, ESA SP 1240, pp. 1–19, 2004.

Newman, C. E., Lewis, S. R., Read, P. L., and Forget, F.: Modeling the Martian dust cycle, 1: Representations of dust transport processes, J. Geophys. Res., 107, 5123, 2002a.

Newman, C. E., Lewis, S. R., Read, P. L., and Forget, F.: Modeling the Martian dust cycle, 2: Multiannual radiatively active dust transport simulations, J. Geophys. Res., 107, 5124, 2002b.

Noe Dobrea, E. Z. and Bell, III, J. F.: TES spectroscopic identification of a region of persistent water ice clouds on the flanks of Arsia Mons Volcano, Mars, J. Geophys. Res., 110, E05 002, doi:10.1029/2003JE002221, 2005.

Ockert-Bell, M. E., Bell, III, J. F., Pollack, J. B., McKay, C. P., and Forget, F.: Absorption and scattering properties of the Martian dust in the solar wavelengths, J. Geophys. Res., 102, 9039–9050, 1997.

Owen, T.: The composition and early history of the atmosphere of Mars, in: Kieffer et al. (1992), pp. 818–834, 1992.

Pearl, J. C., Smith, M. D., Conrath, B. J., Bandfield, J. L., and Christensen, P. R.: Observations of Martian ice clouds by the Mars Global Surveyor Thermal Emission Spectrometer: The first Martian year, J. Geophys. Res., 106, 12 325–12 338, 2001.

Pellinen, R. and Raudsepp, P., eds.: Towards Mars!, Oy Raud Publishing Ltd., helsinki, 2000.

Perrier, S., Bertaux, J. L., Lefevre, F., Lebonnois, S., Korablev, O., Fedorova, A., and Montmessin, F.: Global distribution of total ozone on Mars from SPICAM/MEX UV measurements, J. Geophys. Res., 111, E09S06, doi:10.1029/2006JE002681, 2006.

Pettengill, G. H. and Ford, P. G.: Winter Clouds over the North Martian Polar Cap, Geophys. Res. Lett., 27, 609–612, 2000.

Pickersgill, A. O. and Hunt, G. E.: An examination of the formation of linear lee waves generated by giant Martian volcanoes, J. Atmos. Sci, 38, 40–51, 1981.

Polkko, J., Harri, A.-M., Siili, T., Angrilli, F., Calcutt, S., Crisp, D., Larsen, S., Pommereau, J.-P., Stoppato, P., Lehto, A., Malique, C., and Tillman, J. T.: The NetLander Atmospheric Instrument System (ATMIS): description and performance assessment, Planet. Space Sci., 48, 1407–1420, 2000.

Pollack, J. B., Colburn, D., Kahn, R., Hunter, J., van Kamp, W., Carlston, C. E., and Wolf, M. R.: Properties of aerosols in the Martian atmosphere, as inferred from Viking Lander imaging data, J. Geophys. Res., 82, 4479–4496, 1977.

Pollack, J. B., Colburn, D. S., Flaser, M., Kahn, R., Carlston, C. E., and Pidek, D.: Properties and effects of dust particles suspended in the Martian atmosphere, J. Geophys. Res., 84, 2929–2945, 1979.

Pruppacher, H. R. and Klett, J. D.: Microphysics of Clouds and Precipitation, Kluwer Academic Publishers, 1997.

Read, P. L. and Lewis, S. R.: The Martian Climate Revisited: Atmosphere and environment of a desert planet, Springer, 2004.

Reiss, H.: The Kinetics of Phase Transitions in Binary Systems, J. Chem. Phys., 18, 840–848, 1950.

Renno, N. O., Nash, A. A., Lunine, J., and Murphy, J.: Martian and Terrestrial dust devils: Test of a scaling theory using Pathfinder data, J. Geophys. Res., 105, 1859–1865, 2000.

Rodin, A. V., Clancy, R. T., and Wilson, R. J.: Dynamical properties of Mars water ice clouds and their interactions with atmospheric dust and radiation, Adv. Space Res., 23, 1577–1585, 1999.

Ryan, J. A. and Henry, R. M.: Mars atmospheric phenomena during major dust storms as measured at surface, J. Geophys. Res., 84, 2821–2829, 1979.

Savijärvi, H. and Siili, T.: The Martian slope winds and the nocturnal PBL jet, J. Atmos. Sci., 50, 77–88, 1993.

Savijärvi, H.: Radiative fluxes on a dustfree Mars, Contrib. Atmos. Phys., 64, 103–112, 1991a.

Savijärvi, H.: A model study of the PBL structure on Mars and the Earth, Contrib. Atmos. Phys., 64, 219–229, 1991b.

Savijärvi, H.: Mars Boundary Layer Modeling: Diurnal Moisture Cycle and Soil Properties at the Viking Lander 1 Site, Icarus, 117, 120–127, 1995.

Savijärvi, H.: A model study of the atmospheric boundary layer in the Mars Pathfinder lander conditions, Q.J.R.Meteorol.Soc., 125, 483–493, 1999.

Savijärvi, H.: Surface and boundary layer modeling for the Mars Exploration Rover sites, Q.J.R.Meteorol.Soc., submitted, 2007.

Savijärvi, H. and Vihma, T.: Rajakerroksen fysiikka I, Course material booklet. Yliopistopaino, Helsinki, 61 pages, 2001.

Savijärvi, H., Määttänen, A., Kauhanen, J., and Harri, A.-M.: Mars Pathfinder: new data and new model simulations, Q.J.R.Meteorol.Soc., 130, 669–684, 2004.

Savijärvi, H., Crisp, D., and Harri, A.-M.: Effects of CO_2 and dust on present-day solar radiation and climate on Mars, Q.J.R.Meteorol.Soc., 131, 1–16, 2005.

Schmitt, B., Mulato, L., and Doute, S.: The formation and detectability of CO_2 clathrate hydrate on Mars, in: Proceedings of the Third Mars Polar Science and Exploration conference, LPI Contributions, Lunar and Planetary Institute, Lunar and Planetary Institute, 3600 Bay Area Boulevard, Houston, TX 77058-1113, 2003.

Schofield, J. T., Barnes, J. R., Crisp, D., Haberle, R. M., Larsen, S., Magalhaes, J. A., Murphy, J. R., Seiff, A., and Wilson, G.: The Mars Pathfinder Atmospheric Structure Investigation/Meteorology (ASI/MET) Experiment, Science, 278, 1752–1757, 1997.

Seiff, A. and Kirk, D. B.: Structure of the atmosphere of Mars in summer at mid-latitudes, J. Geophys. Res., 82, 4364–4378, 1977.

Siili, T.: Modeling of albedo and thermal inertia induced mesoscale circulations in the midlatitude summertime Martian atmosphere, J. Geophys. Res., 101, 14 957–14 968, 1996.

Siili, T., Haberle, R. M., and Murphy, J. R.: Sensitivity of Martian southern polar cap edge winds and surface stresses to dust optical thickness and to the large-scale sublimation flow, Adv. Space Res., 19, 1241–1244, 1997.

Siili, T., Haberle, R. M., Murphy, J. R., and Savijärvi, H.: Modelling of the combined late-winter ice cap edge and slope winds in Mars' Hellas and Argyre regions, Planet. Space Sci., 47, 951–970, 1999.

Smith, D. E., Zuber, M. T., Solomon, S. C., Phillips, R. J., Head, J. W., Garvin, J. B., Banerdt, W. B., Muhleman, D. O., Pettengill, G. H., Neumann, G. A., Lemoine, F. G., Abshire, J. B., Aharonson, O., Brown, C. D., Hauck, S. A., Ivanov, A. B., McGovern, P. J., Zwally, H. J., and Duxbury, T. C.: The global topography of Mars and implications for surface evolution, Science, 284, 1495–1503, 1999.

Smith, D. E., Zuber, M. T., Frey, H. V., Garvin, J. B., Head, J. W., Muhleman, D. O., Pettengill, G. H., Phillips, R. J., Solomon, S. C., Zwally, H. J., Banerdt, W. B., Duxbury, T. C., Golombek, M. P., Lemoine, F. G., Neumann, G. A., Rowlands, D. D., Aharonson, O., Ford, P. G., Ivanov, A. B., Johnson, C. L., McGovern, P. J., Abshire, J. B., Afzal, R. S., and Sun, X.: Mars Orbiter Laser Altimeter: Experiment summary after the first year of global mapping of Mars, J. Geophys. Res., 106, 23 689–23 722, 2001a.

Smith, M. D.: The annual cycle of water vapor on Mars as observed by the Thermal Emission Spectrometer, J. Geophys. Res., 107, 5115, 2002.

Smith, M. D.: Interannual variability in TES atmospheric observations in Mars during 1999–2003, Icarus, 167, 148–165, doi:10.1016/j.icarus.2003.09.010, 2004.

Smith, M. D., Pearl, J. C., Conrath, B. J., and Christensen, P. R.: One Martian year of atmospheric observations by the Thermal Emission Spectrometer, Geophys. Res. Lett., 28, 4263–4266, 2001b.

Smith, M. D., Pearl, J. C., Conrath, B. J., and Christensen, P. R.: Thermal Emission Spectrometer results: Mars atmospheric thermal structure and aerosol distribution, J. Geophys. Res., 106, 23 929–23 945, 2001c.

Smith, M. D., Bandfield, J. L., Christensen, P. R., and Richardson, M. I.: Thermal Emission Imaging System (THEMIS) infrared observations of atmospheric dust and water ice cloud optical depth, J. Geophys. Res., 108, 5115, doi: 10.1029/2003JE002115, 2003.

Smith, M. D., Wolff, M. J., Lemmon, M. T., Spanovich, N., Banfield, D., Budney, C. J., Clancy, R. T., Ghosh, A., Landis, G. A., Smith, P., Whitney, B., Christensen, P. R., and Squyres, S. W.: First atmospheric science results from the Mars Exploration Rovers mini-TES, Science, 306, 1750–1753, 2004.

Smith, P. E., Bell, III, J. F., Bridges, N. T., Britt, D. T., Gaddis, L., Greeley, R., Keller, H. U., Herkenhoff, K. E., Jaumann, R., Johnson, J. R., Kirk, R. L., Lemmon, M., Maki, J. N., Malin, C., Murchie, S. L., Oberst, J., Parker, T. J., Reid, R. J., Sablotny, R., Soderblom, L. A., Stoker, C., Sullivan, R., Thomas, N., Tomasko, M. G., Ward, W., and Wegryn, E.: Results from the Mars Pathfinder Camera, Science, 278, 1758–1765, 1997.

Smith, P. H. and Lemmon, M.: Opacity of the Martian atmosphere measured by the Imager for Mars Pathfinder, J. Geophys. Res., 104, 8975–8985, 1999.

Snyder, C. W. and Moroz, V. I.: Spacecraft exploration of Mars, in: Kieffer et al. (1992), pp. 71–119, 1992.

Solomon, S., Qin, D., Chen, M. M. Z., Marquis, M., Averyt, K., Tignor, M., and Miller, H., eds.: Climate Change 2007: The Physical Science Basis. Contribution of Working Group I to the Fourth Assessment Report of the Intergovernmental Panel on Climate Change, Cambridge University Press, Cambridge, United Kingdom and New York, NY, USA, 996 pp., 2007.

Spiga, A., Forget, F., Dolla, B., Vinatier, S., Melchiorri, R., Drossart, P., Gendrin, A., Bibring, J.-P., Langevin, Y., and Gondet, B.: Remote sensing of surface pressure on Mars with the Mars Express/OMEGA spectrometer: 2. Meteorological maps, J. Geophys. Res., 112, E08S16, doi:10.1029/2006JE002870, 2007.

Stauffer, D.: Kinetic theory of two-component ('Heteromolecular') nucleation and condensation, J. Aerosol Sci., 7, 319–333, 1976.

Stull, R. B.: An introduction to boundary-layer meteorology, Kluwer, Dordrecht, 1988.

Sutton, J. L., Leovy, C. B., and Tillman, J. E.: Diurnal variations of the Martian surface layer meteorological parameters during the first 45 sols at two Viking Lander sites, J. Atmos. Sci., 35, 2346–2355, 1978.

Tamppari, L. K.: The Phoenix Mars Scout Mission, in: Desjean et al. (2006), p. 7.1.4., 2006.

Tamppari, L. K., Zurek, R. W., and Paige, D. A.: Viking era water-ice clouds, J. Geophys. Res., 105, 40 879–4107, 2000.

Tamppari, L. K., Zurek, R. W., and Paige, D. A.: Viking-era diurnal water-ice clouds, J. Geophys. Res., 108, 5073, 2003.

Taylor, F. W., Calcutt, S. B., Read, P. L., Lewis, S. R., McCleese, D. J., Schofield, J. T., and Zurek, R. W.: Atmospheric temperature sounding on Mars and the climate sounder on the 2005 reconnaissance orbiter, Adv. Space Res., 38, 713–717, 2005.

Thomas, P. and Gierasch, P. J.: Dust devils on Mars, Science, 230, 175–177, 1985.

Tillman, J. E.: Mars global atmospheric oscillations: annually synchronized, transient normal-mode oscillations and the triggering of global dust storms, J. Geophys. Res., 93, 9433–9451, 1988.

Tillman, J. E., Henry, R. M., and Hess, S. L.: Frontal systems during passage of the Martian North polar hood over the Viking Lander 2 site prior to the first 1977 dust storms, J. Geophys. Res., 84, 2947–2954, 1979.

Tillman, J. E., Johnson, N. C., Guttorp, P., and Percival, D. B.: The Martian annual armospheric pressure cycle: years without great dust storms, J. Geophys. Res., 98, 10 963–10 971, 1993.

Tillman, J. E., Landberg, L., and Larsen, S. E.: The boundary layer of Mars: fluxes, stability, turbulent spectra, and growth of the mixed layer, J. Atmos. Sci., 51, 1709–1727, 1994.

Titov, D. V., Markiewicz, W. J., Thomas, N., Keller, H. U., Sablotny, R. M., Tomasko, M. G., Lemmon, M. T., and Smith, P. H.: Measurements of the atmospheric water vapor on Mars by the Imager for Mars Pathfinder, J. Geophys. Res., 104, 9019–9026, 1999.

Tobie, G., Forget, F., and Lott, F.: Numerical simulation of the winter polar wave clouds observed by Mars Global Surveyor Mars Orbiter Laser Altimeter, Icarus, 164, 33–49, 2003.

Tomasko, M. G., Loose, L. R., Lemmon, M., Smith, P. H., and Wegryn, E.: Properties of dust in the Martian atmosphere from the Imager of Mars Pathfinder, J. Geophys. Res., 104, 8987–9007, 1999.

Trinkaus, H.: Theory of the nucleation of multicomponent precipitates, Phys. Rev. B., 27, 7372–7378, 1983.

Vasquez, L. and Gomez-Elvira, J.: The rover environmental monitoring station (REMS) of the Mars Science Laboratory (MSL, NASA/JPL 2009), in: Desjean et al. (2006), p. 7.2.1., 2006.

Vehkamäki, H.: Classical Nucleation Theory in Multicomponent Systems, Springer, Berlin Heidelberg, 2006.

Volmer, M.: Kinetik der Phasenbildung, Steinkopff, Dresden und Leipzig, 1939.

Wagner, P., Kaller, D., Vrtala, A., Lauri, A., Kulmala, M., and Laaksonen, A.: Nucleation probability in binary heterogeneous nucleation of water-n-propanol vapor mixtures on insoluble and soluble nanoparticles, Phys. Rev. E, 67, 021 605, 2003.

Wang, H. and Ingersoll, A. P.: Martian clouds observed by Mars Global Surveyor Mars Orbiter Camera, J. Geophys. Res., 107, 5078, doi:10.1029/2001JE001815, 2002.

Withers, P. and Smith, M. D.: Atmospheric entry profiles from the Mars Exploration Rovers Spirit and Opportunity, Icarus, 185, 133–142, doi:10.1016/j.icarus.2006.06.013, 2006.

Wolff, M. J. and Clancy, R. T.: Constraints of the size of Martian aerosols from Thermal Emission Spectrometer observations, J. Geophys. Res., 108, 5097, doi:10.1029/2003JE002057, 2003.

Wolff, M. J., Bell, III, J. F., James, P. B., Clancy, R. T., and Lee, S. W.: Hubble Space Telescope observations of the Martian aphelion cloud belt prior to the Pathfinder mission: Seasonal and interannual variations, J. Geophys. Res., 104, 9027–9041, 1999.

Wood, S. E.: Nucleation and Growth of CO_2 Ice Crystals in the Martian Atmosphere, Ph.D. thesis, University of California, Los Angeles, 1999.

Wood, S. E., Schneider, M. A., Cardell, G., Hecht, M., knowlen, C., Bruckner, A. P., Catling, D. C., Cobos, D., and Zent, A.: Characterization and calibration of the Phoenix TECP relative humidity sensor in a Mars atmospheric simulation chamber, in: Fourth international conference on Mars polar science and exploration, LPI Contributions, p. 8080, Lunar and Planetary Institute, Lunar and Planetary Institute, 3600 Bay Area Boulevard, Houston, TX 77058-1113, 2006.

Ye, Z. J., Segal, M., and Pielke, R. A.: A comparative study of daytime thermally induced upslope flow on Mars and Earth, J. Atmos. Sci., 47, 612–628, 1990.

Zasova, L., Formisano, V., Moroz, V., Grassi, D., Ignatiev, N., Giuranna, M., Hansen, G., Blecka, M., Ekonomov, A., Lellouch, E., Fonti, S., Grigoriev, A., Hirsch, H., Khatuntsev, I., Mattana, A., Maturilli, A., Moshkin, B., Patsaev, D., Piccioni, G., Rataj, M., and Saggin, B.: Water clouds and dust aerosols observations with PFS MEX at Mars, Planet. Space Sci., 53, 1065–1077, 2005.

Zent, A. P., Haberle, R. M., Houben, H. C., and Jakosky, B. M.: A coupled subsurface-boundary layer model of water on Mars, J. Geophys. Res., 98, 3319–3337, 1993.

Zurek, R. W. and Smrekar, S. E.: An overview of the Mars Reconnaissance Orbiter (MRO) science mission, J. Geophys. Res., 112, E05S01, doi:10.1029/2006JE002701, 2007.

Zurek, R. W., Barnes, J. R., Haberle, R. M., Pollack, J. B., Tillman, J. E., and Leovy, C. B.: Dynamics of the atmosphere of Mars, in: Kieffer et al. (1992), pp. 835–934, 1992.